PERFORMANCE AND OPERABILITY OF A DUAL CAVITY FLAME HOLDER IN A SUPERSONIC COMBUSTOR

THESIS

MacKenzie J. Collatz, First Lieutenant, USAF

AFIT/GSS/ENY/09-J01

DEPARTMENT OF THE AIR FORCE
AIR UNIVERSITY

AIR FORCE INSTITUTE OF TECHNOLOGY

Wright-Patterson Air Force Base, Ohio

The views expressed in this thesis are those of the author and do not reflect the official policy or position of the United States Air Force, Department of Defense, or the United States Government.

AFIT/GSS/ENY/09-J01

PERFORMANCE AND OPERABILITY OF A DUAL CAVITY FLAME HOLDER IN A SUPERSONIC COMBUSTOR

THESIS

Presented to the Faculty

Department of Aeronautics and Astronautics

Graduate School of Engineering and Management

Air Force Institute of Technology

Air University

Air Education and Training Command

In Partial Fulfillment of the Requirements for the

Degree of Master of Science (Space Systems)

MacKenzie J. Collatz

First Lieutenant, USAF

June 2009

AFIT/GSS/ENY/09-J01

PERFORMANCE AND OPERABILITY OF A DUAL CAVITY FLAME HOLDER IN A SUPERSONIC COMBUSTOR

MacKenzie J. Collatz

First Lieutenant, USAF

June 2009

Approved:

/signed/	3 June 2009
Lt Col Richard Branam, USAF (Chairman)	date
/signed/	3 June 2009
Dr. Mark Gruber (Member)	date
/signed/	8 June 2009
Dr. Paul King (Member)	date

Abstract

Supersonic combustion has been of interest for many years in order to support future Air Force hypersonic missions. The current generation of hydrocarbon fueled scramjet combustors typically requires a flame holding device to facilitate flame ignition and stable combustion. The amount of time available for fuel injection, fuel-air mixing, and combustion is very short, on the order of 1 millisecond. This short dwell time, along with the relatively long ignition delay times of hydrocarbon fuels, makes the flow path and flame holder design extremely important. This study investigates the performance and operability of using a symmetric dual cavity flame holder flow path to stabilize and enhance supersonic combustion. Testing of this flow path configuration, as well as a baseline single cavity flow path, was conducted in Research Cell 18 of the Propulsion Directorate at the Air Force Research Laboratory (AFRL/RZ). Multiple flight conditions, equivalence ratios, and fueling schemes were studied. Performance and operability of the flow paths were determined through analysis of wall pressures, temperatures, pressure ratios, stream thrusts, combustion efficiencies, computational fluid dynamics, and visualization. The dual cavity flame holder showed a significant overall increase in performance through higher temperatures, pressure ratios, and stream thrusts. The operability was slightly reduced due to an increase in pre-combustion shock train position. CFD and flow path visualization were used to verify these results. This research has proven the potential of a dual cavity flame holder to provide improved performance for a reliable scramjet engine.

Acknowledgements

I would like to express my sincere gratitude to my faculty advisor, Lt Col Richard Branam, for his guidance and assistance throughout this study and my coursework at AFIT. I would also like to thank my sponsor, Dr. Mark Gruber, for his mentorship during this work and for the past three years. It has been a pleasure and honor to work with and learn from you throughout my time in the Propulsion Directorate. Thank you to the management at AFRL/RZA who provided me with this opportunity to advance my education and supported the testing of this research.

Many thanks go to the crew of Research Cell 18, including Dr. Steven Lin, Matt Streby, Lt Dell Olmstead, Lt John Heaton, Paul Kennedy, Tim Bulcher, Steve Enneking, and Dr. Skip Williams. I appreciate all of your hard work and dedication through the months of late run nights. I could not have asked for a better group of people to work with. I am also extremely indebted to Dr. John Tam for the countless hours of support and guidance he has provided.

Finally, I would like to thank my family and my fiancé for their endless love and encouragement. Your constant support of my career and education means more than you know. None of this would ever have been possible without you.

Table of Contents

Page

List of Figures

Page

List of Tables

Page

List of Symbols

Symbol	
A	Area (in^2)
F	Load cell force (lb_f)
H	Enthalpy (Btu/lb_m)
MW	Molecular weight (amu)
n	Number of measurements
P	Pressure (psia)
Q	Heat loss (Btu/sec)
R_U	Universal gas constant ($ft\text{-}lb_f/R \cdot lb_m\text{-}mol$)
ST	Stream thrust (lb_f)
T	Temperature (R)
U	Velocity (ft/s)
W	Mass flow rate (lb_m/s)
Y_{FROZ}	Mass fraction of frozen fuel
ρ	Density (lb_m/in^3)
η_c	Combustion efficiency
ϕ	Equivalence ratio
σ	Standard deviation

Subscripts:	
4	Facility nozzle exit station
5	Combustor exit
amb	Ambient
base	Combustor base
inj	Injector
T	Total

List of Abbreviations

Abbreviation	
AFIT	Air Force Institute of Technology
AFRL	Air Force Research Laboratory
ER	Equivalence Ratio
L/D	Length to Depth Ratio
RZ	Propulsion Directorate of the Air Force Research Laboratory
WPAFB	Wright-Patterson Air Force Base

PERFORMANCE AND OPERABILITY OF A DUAL CAVITY FLAME HOLDER IN A SUPERSONIC COMBUSTOR

I Introduction

I.1 Motivation

Future hypersonic aerospace systems will provide the warfighter with revolutionary capabilities to project force anywhere, anytime (1). Scramjet engines will enable three categories of hypersonic crafts: weapons, such as hypersonic cruise missiles; aircraft, such as those designed for global strike and reconnaissance missions; and space vehicles, as part of a reusable access to space platform. The scramjet will power vehicles hundreds of miles in just minutes, and will make rapid global travel and affordable access to space a reality (2). These capabilities will support the United States Air Force mission by providing the warfighter with the most advanced weaponry, aircraft, and space access, all in shorter timeframes than ever previously possible.

Supersonic combustion is of broad national and international interest, especially as it relates to the development and fielding of scramjet engines for these hypersonic missions. Efficient fuel injection and mixing is a primary area of study for the current generation of hydrocarbon-fueled scramjet combustors. Combustors typically require a flame holding device in the fixed flow path to facilitate flame ignition and stable combustion, due to the relatively long ignition delay times of hydrocarbon fuels. A primary area of study has been the development of a recessed cavity flame holder. On-going experimentation at the Air Force Research Laboratory's Propulsion Directorate

aims to improve the flow path design by enhancing flame holders such as these. Research has shown improved performance and operability with a single cavity placed on the top side of the flow path. Computational studies have also shown positive effects of adding an additional cavity flame holder directly below the first one on the bottom side of the flow path (3). However, no physical dual cavity flow path has ever been studied experimentally in a supersonic testing facility in the United States. The goal of this research is to compare a single cavity flame holding flow path with that of a dual cavity, both being tested in a supersonic combustion research rig at AFRL/RZ at Wright-Patterson Air Force Base (WPAFB), Ohio.

This dual cavity flow path has been incorporated into the vehicles of the joint US and Australian Hypersonic International Flight Research Experimentation (HIFiRE) Program (3). The program aims to study basic hypersonic phenomena and will begin flight testing in May 2009. The current research, along with future HIFiRE flight test data, will provide significant insight into the capabilities of this flow path.

I.2 Problem Statement

Previous research has been conducted to study various scramjet flow paths to improve combustion efficiency and performance (3-8). One possible flow path configuration includes the use of symmetrical cavity flame holders; however, this configuration has only been studied using computational methods. Actual flow path hardware has been developed by the Air Force Research Laboratory and was experimentally studied in this research. The results of this testing were used in

conjunction with computational analysis, conducted by members of AFRL/RZ, to provide performance and operability results that have been previously unavailable.

I.3 Research Objectives

The first objective of this research was to investigate dual cavity performance and to determine the advantages and disadvantages of using a dual cavity versus a single cavity flame holder. The second objective was to investigate the operability of the dual cavity over a range of equivalence ratios and fuel injection schemes. The final objective was to compare the benefits and disadvantages of the two flow path configurations and to determine if the dual cavity flame holder may be a viable option for future scramjet engines.

I.4 Research Focus

The focus of this research was to design a test matrix with a wide range of conditions, to carry out these tests, and to analyze the results. The run conditions included two primary flight conditions, equivalence ratios ranging from 0.3 to 1.1, and several combinations of fuel injection sites. This research focused specifically on the data collection and analysis process. All hardware and code used for this study was pre-existing.

The question this research answers is: does a dual cavity flow path hold significant advantages over a similar flow path with only a single cavity flame holder? Data was collected and analyzed to determine the combustion efficiencies, stream thrusts, pressure profiles, and shock train positions of each of the two configurations. These

results were studied to determine overall performance and operability of the two flow paths.

II Theory and Previous Research

II.1 Supersonic Ignition

Supersonic combustion has been of interest for many years in order to support future hypersonic missions. However, it has proven to be a very complex area of study with many challenges. The current generation of hydrocarbon fueled scramjet combustors typically requires a flame holding device to facilitate flame ignition and stable combustion. The amount of time available for fuel injection, fuel-air mixing, and combustion is very short, on the order of 1 millisecond. This short dwell time, along with the relatively long ignition delay times of hydrocarbon fuels, makes the flow path and flame holder design extremely important (4). Research conducted by Liu, et al. investigated this challenge through the use of computational fluid dynamics modeling. Cavity-stabilized ethylene-air flames were simulated to predict flame-stability limits in supersonic flows using reduced chemical kinetic mechanisms based on experimental studies. Several fuel flow rates were considered, and combustion in the cavity involved fuel-lean and fuel-rich conditions. CFD code was used to predict the ignition delay times for an auto-ignition problem using a wide range of initial temperatures, pressures, and equivalence ratios. The study showed that as the pressure was decreased, the ignition delay times increased, and that as the temperature was decreased, the ignition delay times increased. It also showed that as equivalence ratio was increased, the delay times decreased (5).

II.2 Cavity Flame Holder Design

The scramjet community has proposed the use of cavity flame holders to stabilize and enhance supersonic combustion. The main purpose is to create a subsonic recirculation region inside the cavity with a hot pool of radicals, which will reduce the induction time (6). This will allow autoignition of the fuel/air mixture to take place. Over recent years, the design of cavity flame holders has been extensively studied (7).

Proper dimensions are critical to cavity performance. If deep enough, the cavity will offer a relatively long residence time for mixing and chemical reactions to take place. Cavity geometries are typically defined by their length to depth ratio (L/D). A general cavity geometry is shown in Figure 1.

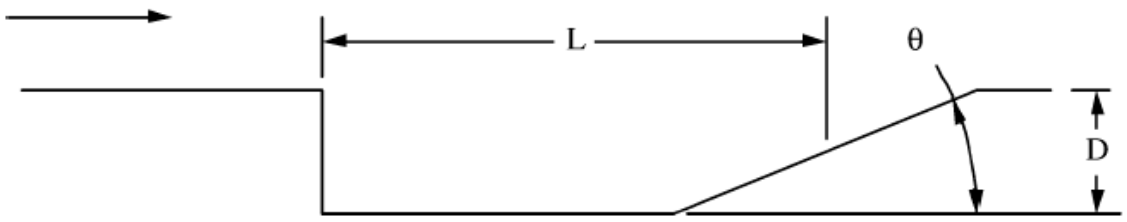

Figure 1: General cavity geometry (8)

A cavity is considered open if it has an L/D of less than 7-10. Open cavities are characterized by a reattachment of a shear layer to the rear step. If the value for L/D is great enough (larger than 10-13), the shear layer reattaches to the cavity floor and the cavity is termed closed (7). Closed cavities commonly suffer from severe drag penalties and are rarely used. In open cavities, a shear layer forms between the high momentum

core flow and the subsonic flow within the cavity. This shear layer is unsteady and impinges on the rear wall allowing mass to enter. The cavity pressure then increases and creates self-sustaining longitudinal pressure oscillations resulting in drag (9). The resonance may be controlled and stabilized by slanting the back wall at an angle as shown in Figure 1 (10).

II.3 Fuel Injection

Several investigations over the past decade have examined the utility of wall cavities as flame holders for liquid and gaseous-fueled scramjet combustors (7). Fuel injection placement has been one primary area of study. Fuel can be introduced into the cavity either by entrainment from the freestream when injection occurs upstream of the cavity, or through direct injection. In all cases, the cavity entrains oxidizer from the freestream. Additionally, because the cavity is characterized by a relatively high recovery factor the total temperature of the mixture within the cavity is close to the total temperature of the freestream near the cavity (11). Therefore, if operated with a desirable fuel-air mixture, favorable conditions are likely to exist within the cavity to sustain combustion.

II.4 Flow Field Variations

Another main challenge of flame holder design in hydrocarbon-fueled scramjets is the changing character of the flow field depending on the operating mode of the combustor. The combustor flow is primarily supersonic prior to ignition. Assuming

ignition takes place at a relatively low flight Mach number, the combustor is then characterized by dual-mode operation where a strong pre-combustion shock train exists. This system of shock waves creates a distorted flow field containing regions of both subsonic and supersonic flow. As the vehicle accelerates to higher Mach numbers, the shock train weakens, and the flow field through the engine returns to supersonic conditions. Figure 2 shows two representative shadowgraph images that illustrate the flow field with and without a shock train.

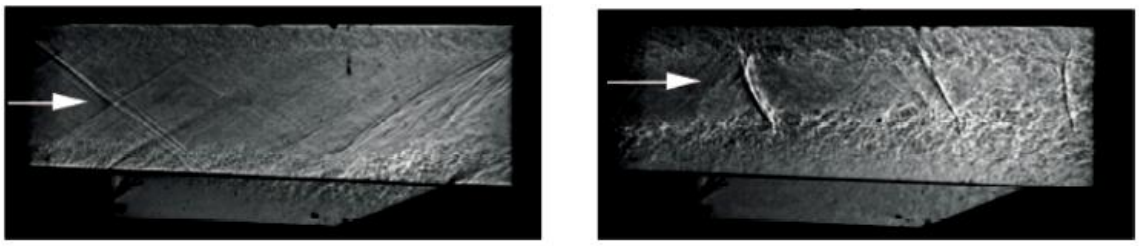

Figure 2: Shadowgraph images with (left) and without (right) a shock train (8)

A robust flame holder must be able to tolerate the flow field changes without losing effectiveness. Figure 3 shows the mixing of an ethylene jet in a clean and distorted supersonic flow.

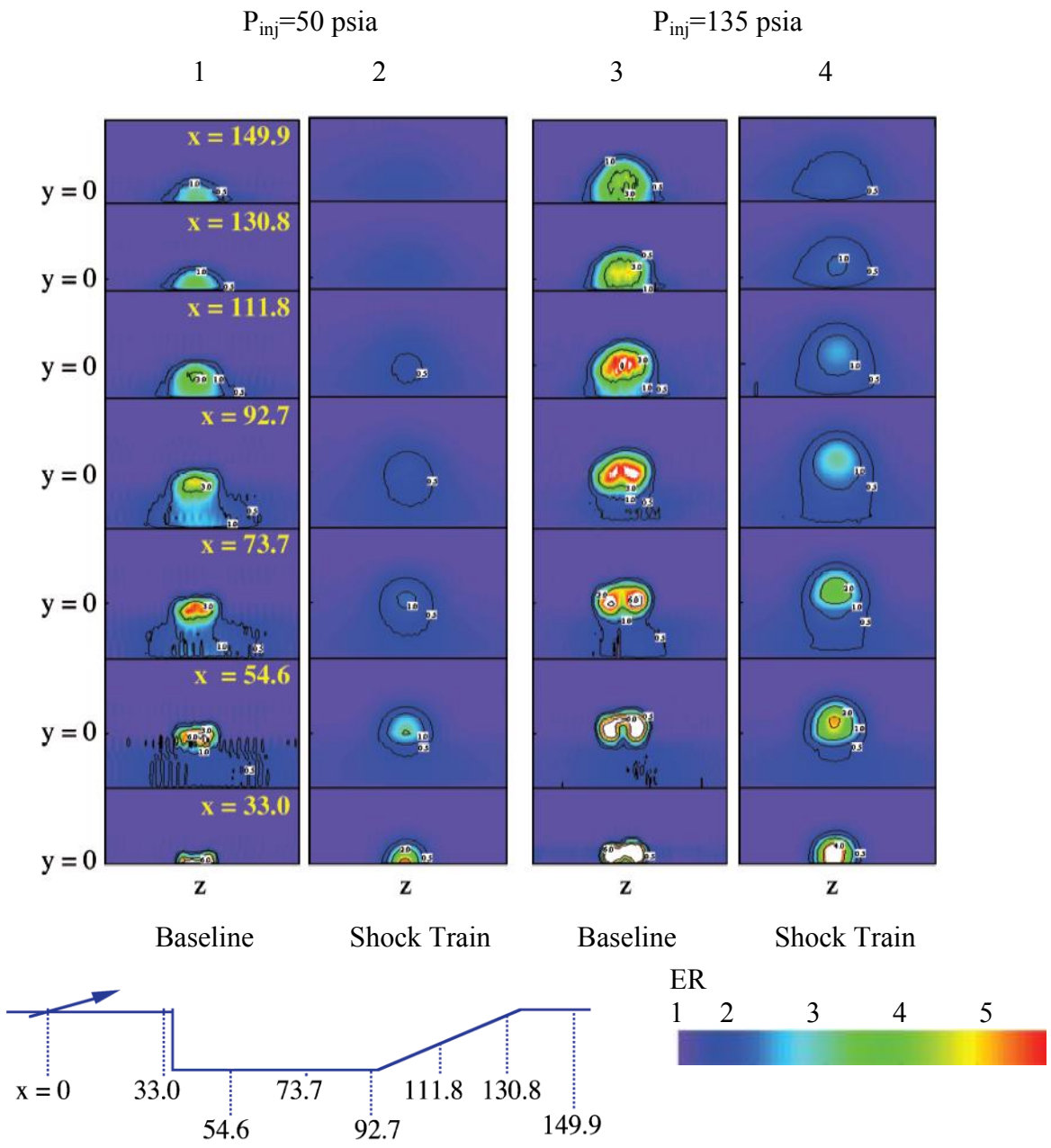

Figure 3: Mixing of an ethylene jet in a clean (baseline) and distorted (shock train) supersonic flow (8)

Columns 1 and 3 represent low backpressure cases for clean supersonic flow (baseline). Columns 2 and 4 have a higher backpressure leading to a distorted flow field (shock train). In these images, the flow direction is out of the page, and all axial positions are in millimeters. The fuel plume penetrates higher into the main stream as the injection

pressure is increased. Counter-rotating streamwise vortical structures are observed near the injector when the gas is injected into the clean supersonic flow. As the backpressure is increased, a normal shock train develops in the flow, leading to a highly distorted flow field with boundary layer separation. As the fuel jet encounters the distorted flow, the fuel plume changes radically. The imposed shock system also elevates the fuel plume away from the wall, potentially affecting the stability of the flame holder by altering the entrainment of fuel and air into the cavity (8).

II.5 Experimental and Flight Test Background

Most researchers agree that the use of these cavities provides a viable option to overcome the mixing and flame holding challenges of supersonic combustors. Experimental and computational results suggest excellent performance can be achieved with the use of a cavity flame holder along with the proper fueling scheme. However, to date, all experimental data has been collected while using only a single cavity flame holder. Computational research at the Propulsion Directorate at Wright-Patterson Air Force Base studied the possibility of adding a second cavity to the flow path (3). This option was considered during the design of the flow path for the Hypersonic International Research Experimentation Program. The HIFiRE Program is a joint effort between the US Air Force Research Laboratory and the Australian Defense Scientific and Technology Organization. It is devoted to studying basic hypersonic phenomena through flight experimentation. Due to payload integration concerns, the combustor flow path was shortened, and a duplicate cavity flame holder was added to the bottom side of the flow

path, while all other features were preserved. This modification was incorporated to offset potential effects of the reduced combustor length and to more effectively utilize the centerline flow path configuration allowing both top and bottom walls to be used for flame holding. Computational analyses showed a dramatic improvement in combustor performance over the original single cavity design (3). Hardware for this type of flow path was then designed and manufactured for future testing in the research cells of AFRL. This hardware, shown in Figure 4, and a similar flow path design are the focus of the present study.

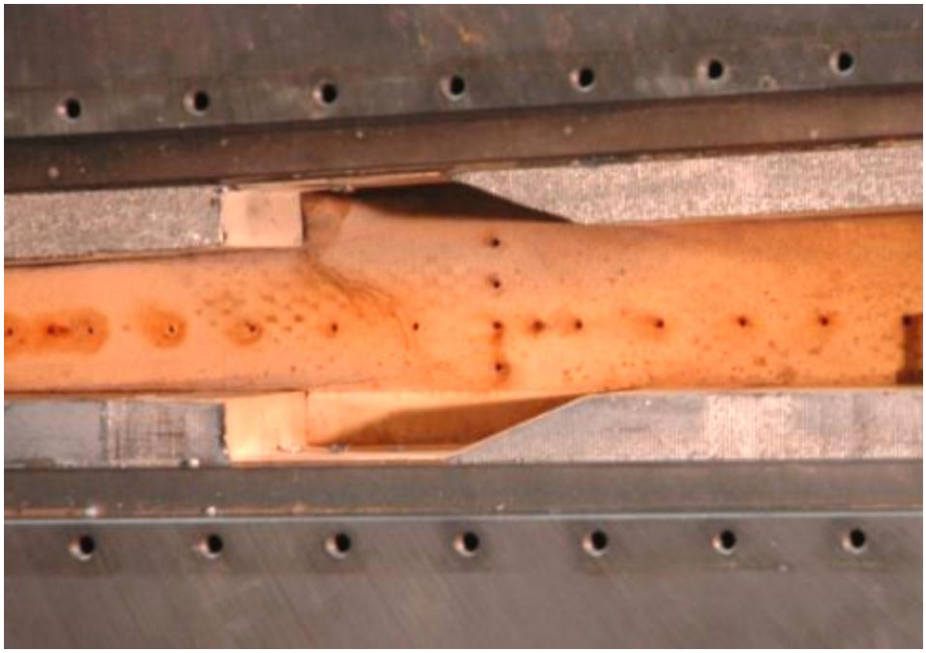

Figure 4: Photograph of the dual cavity flow path; flow from left to right

III Test Setup and Apparatus

III.1 Test Facility

This experiment was carried out in Research Cell 18, a supersonic combustion facility located in the Propulsion Directorate at Wright-Patterson Air Force Base. The facility was designed for fundamental studies of supersonic reacting flows using a continuous-run, direct-connect, open-loop air flow supported by the Research Air Facility. The main components of the research rig include a natural-gas-fueled vitiator, an interchangeable facility nozzle, a modular isolator, a modular combustor, and an exhaust pipe. Figure 5 below is a photograph of the research rig and Figure 6 is a diagram showing each of the main components with air flowing from left to right.

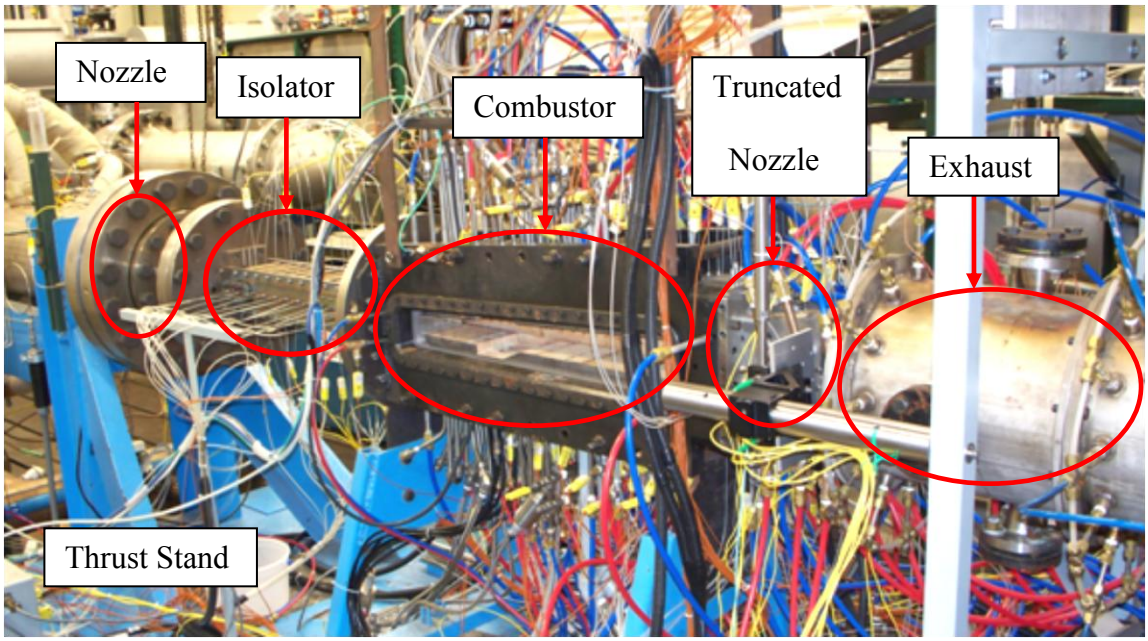

Figure 5: Photograph of Research Cell 18 rig

The rig is mounted on a thrust stand capable of measuring up to 2000 lb_f of thrust. The Research Air Facility utilizes a series of compressors to provide up to 30 lb/s of air with pressures and temperatures up to 750 psia and 1600 R, respectively. The exhaust system provides pressure as low as 3.5 psia to lower and maintain the backpressure for smooth starting and safe operation. Two nozzles, a Mach 1.8 and a Mach 2.2, are currently available to generate appropriate supersonic flow conditions upstream of the combustor flow path. These nozzles, along with the air vitiator, can simulate discrete flight conditions between Mach 3.5 and Mach 5.0 with flight dynamic pressures up to 2000 psf. These flight conditions represent the approximate Mach numbers where the engine transitions from dual-mode, where both subsonic and supersonic combustion can occur, to pure scramjet mode where the combustion is always supersonic (4).

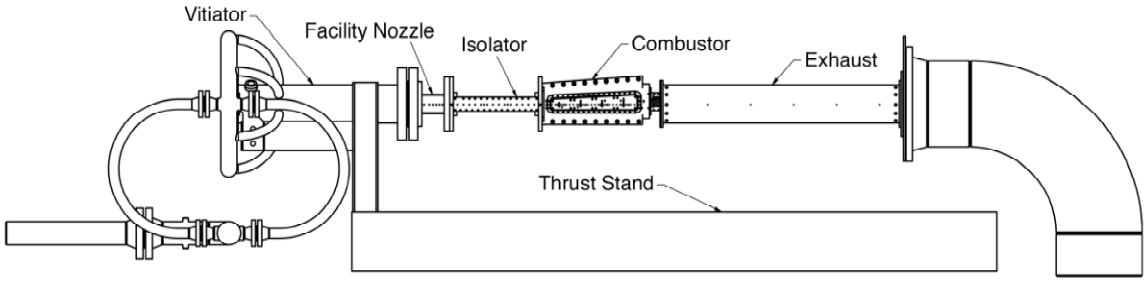

Figure 6: Schematic of Research Cell 18 combustion facility at WPAFB (4)

The flow path can be configured in a variety of ways. The single and dual cavity flow path setups used in this study are shown in Figure 7. The baseline flow path for this experiment consists of a heat-sink rectangular isolator and a rectangular combustor. The isolator has a constant area, while the combustor features a top side recessed cavity flame

holder and an expanding top wall. The dual cavity configuration is identical to the single cavity flow path, but with a symmetric second cavity installed directly below the top side cavity. The flow path contains four separate fuel injection sites, all with three and four hole injection options per site. I-2 and I-4 are located upstream of the cavities, on the top and bottom walls, respectively, while I-5 and I-7 are downstream on the top and bottom sides, respectively. I-5 and I-7 are normal to the flow and I-2 and I-4 are low angle injectors. The combustor hardware contains multiple other fuel injection options that were not studied during this experiment. Room temperature ethylene was the fuel used for all runs.

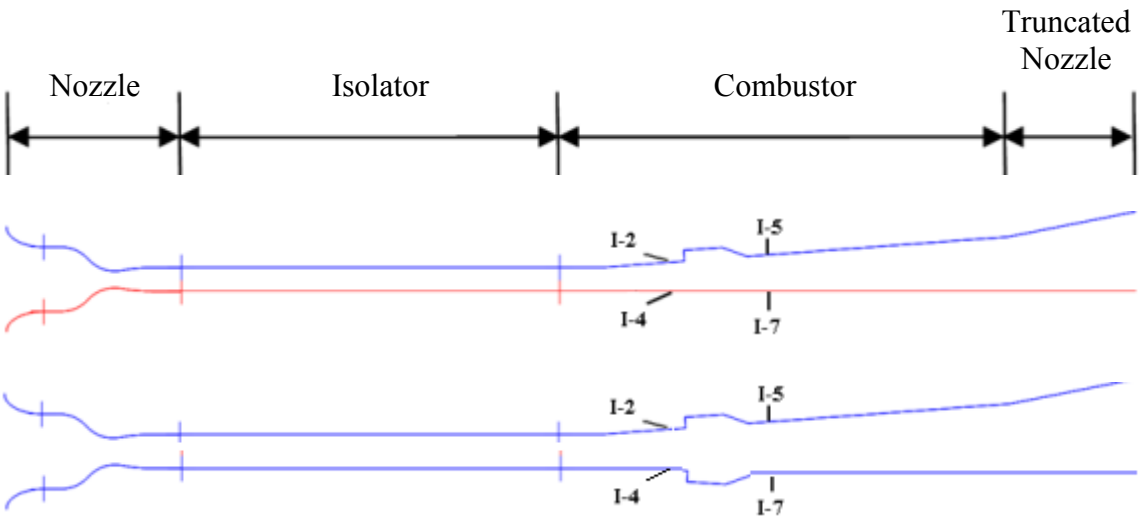

Figure 7: Research Cell 18 single and dual cavity flow paths

The isolator has a height of 1.5 in, a width of 4.0 in, and a length of 25.75 in. The combustor is 26 in long with a constant divergence angle of 2.6 degrees (12). The rig is water-cooled and the entire flow path is covered with thermal barrier coating for additional thermal protection. The south wall of the combustor can be replaced with a

quartz window allowing flame visualization and optical measurements. The cavities span the entire flow path width and are each 0.675 in deep and 4.173 in long, including a forward-facing ramp. Two conventional spark plugs are located in each cavity and are used as the primary means of ignition. Aerothrottle slots are located just downstream of the cavities to assist in ignition when necessary. Aerothrottle is the process of injecting compressed air downstream of the cavity to generate a pre-combustion shock train, raising the pressure and temperature in the combustor allowing ignition to occur. Figure 8 shows the combustor dimensions for the dual cavity flow path along with the locations of the circular windows that can be installed.

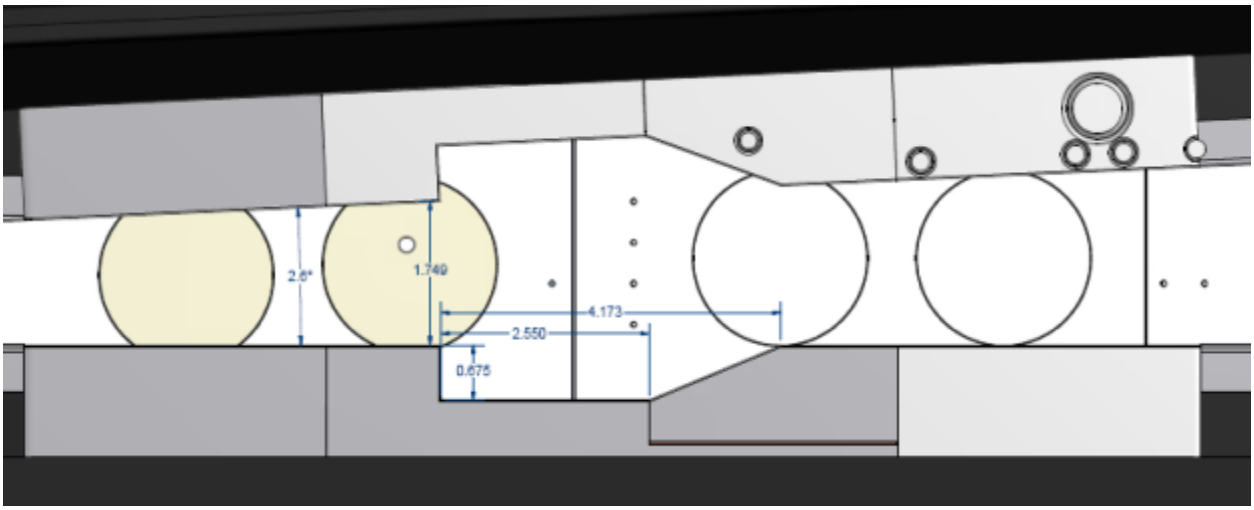

Figure 8: Side view of the flow path showing the dual flame holding cavities on the top and bottom walls; flow from left to right

III.2 Basic Instrumentation

Thermocouple ports and pressure taps are located throughout the flow path for instrumentation and health monitoring. The data acquisition system consists of a

CAMAC-based crate with 128 analog inputs, 16 analog outputs, 48 digital inputs, and 32 digital output channels. There is also a 256-channel electric pressure and a 64-channel thermocouple scanning system. Instrumentation readings from thermocouples and pressure transducers, as well as various other measurement devices, were recorded at a frequency of 2-10 Hz. Conventional and high-speed cameras were used for flame visualization when quartz windows were installed.

III.3 Test Procedures

The author planned an extensive set of test conditions. These included hundreds of runs with various configurations of facility nozzles, dynamic pressures, inlet temperatures and pressures, fueling combinations, and equivalence ratios. Mach 1.8 and Mach 2.2 facility nozzles were used, but only Mach 2.2 cases were specifically analyzed. Dynamic pressures ranged between 500 and 2000 psf. Inlet temperatures and pressures were between 960 and 1828 R and 51.4 to 208.3 psia, respectively. A variety of fueling schemes were used including different combinations of up and downstream injection sites, as well as top and bottom wall sites.

Testing was conducted over nine nights throughout a three-month period. Due to installation efforts, only one nozzle configuration could be tested each night, but all other conditions could be varied with relative ease. Approximately seven people were required to run the rig each night, as well as an additional two to three to run the air facility. The roles of each team member in the test cell varied, but the entire process required a great deal of teamwork. Responsibilities of some of the individuals included: coordinating the

facility checklist, monitoring the systems for health and fire, and running systems such as the aerothrottle control, the vitiator control, data acquisition systems, and the combustor fuel control. The author's primary responsibilities included managing the test matrix, running diagnostic systems, and overseeing the entire testing process.

Each run began with a start up of the vitiator with a short period of air flowing without any fuel. This time was used to insure that all test conditions had been met. Fuel was then injected and spark plugs were used for ignition. If no ignition took place, an aerothrottle was used. Many cases would not ignite, even with the use of the aerothrottle. This is the primary indicator for determining the operability window of each configuration. During runs with successful ignition, approximately 10-15 seconds of data was taken. The data acquisition system runs continually, and therefore acquires all segments of the run from start up through shut down. Over a three-month testing period, 216 runs were conducted. This totaled over 1.5 GB of data. In order to keep the amount of data reduction to an acceptable level, yet still provide a thorough analysis, 14 runs were selected for direct comparison. The runs were separated into cases, each case with one single cavity and one dual cavity run. The runs for each case were chosen due to their similar flight conditions and total equivalence ratios. The first three cases used only the I-2 fuel injector. Each run in cases 4-7 had the same primary, secondary, and total equivalence ratio as the other run in its case, but made use of multiple injectors. For the single cavity runs in these cases, only top side fuel injection was used. However, for the dual cavity runs, both top and bottom side fueling was used. Table 1 shows the conditions for each case.

Table 1: Experimental Test Cases

Case	Cavity	Run	Q (psf)	Flight M	I-2	I-4	I-5	I-7	Total ER
1	Single	295AB	500	4.5	0.6				0.6
1	Dual	329AM	500	4.5	0.6				0.6
2	Single	295AK	500	4.5	0.9				0.9
2	Dual	329AN	500	4.5	0.9				0.9
3	Single	295AL	500	4.5	1.1				1.1
3	Dual	329AO	500	4.5	1.1				1.1
4	Single	297AD	500	4.5	0.6				0.6
4	Dual	329AR	500	4.5	0.3	0.3			0.6
5	Single	295AM	500	4.5	0.6				0.6
5	Dual	323AN	500	4.5	0.3	0.3			0.6
6	Single	297AW	1000	5.0	0.6				0.6
6	Dual	319AD	1000	5.0	0.3	0.3			0.6
7	Single	297AX	1000	5.0	0.45		0.45		0.9
7	Dual	319AJ	1000	5.0	0.225	0.225	0.225	0.225	0.9

The first three numbers of the run identification number are the Julian calendar date for 2008. The two following letters state the order of the runs for that particular night (i.e. run AA is the first run, run AB is the second, and so on). Each of these runs were conducted using the Mach 2.2 nozzle and had dynamic pressures of either 500 or 1000 psf. These relate to flight conditions of Mach 4.5 and 5.0, respectively.

Table 1 shows the nominal equivalence ratio values. The actual equivalence ratios were later determined by taking the average of the ratio of air and fuel flow rates output by the system over the period of steady state combustion and dividing by the stoichiometric fuel to air ratio for ethylene, 0.06792. The air and fuel flow rates were found using mass flow meters that both measure and control the flows.

III.4 Data Analysis Process

The data from each run night was output into a spreadsheet. The first step in the analysis process was to take each of these spreadsheets and format them into a more user-friendly form. Each run night was broken down into its respective runs, and the 14 cases for primary comparisons were extracted. The data required for analysis from each run was separated out. A master spreadsheet was then created for each run. This included all necessary information required for the analysis of pressures, temperatures, flow rates, efficiencies, thrusts and stream thrusts, as well as general information for the run. Time, date, and nominal test conditions were extracted. Readings for approximately 190 pressure taps and 40 thermocouples were saved, along with multiple air and fuel flow rates, two load cell readings, and aerothrottle control information.

The relevant times for each run then had to be acquired from the data set. The data acquisition system output readings five times every second. Each reading taken while fuel was flowing was saved, as well as several seconds of data prior to the start when only air was flowing. The few seconds of steady state combustion was identified for each run by analyzing the pressure tap readings near the center of the combustor in the top side cavity. This tap was assumed the one with the greatest pressure rise. The

pressure began low, dramatically increased during ignition, and then leveled off during steady state combustion before rapidly decreasing at fuel shut-off. This time period of steady state combustion, minus several readings on each end, was considered the time of good combustion and was used as the range for analysis for all other performance parameters. From this point, each operability and performance parameter was individually studied.

For analysis of the cavity combustion, temperature profiles were plotted. An example is shown in Figure 9.

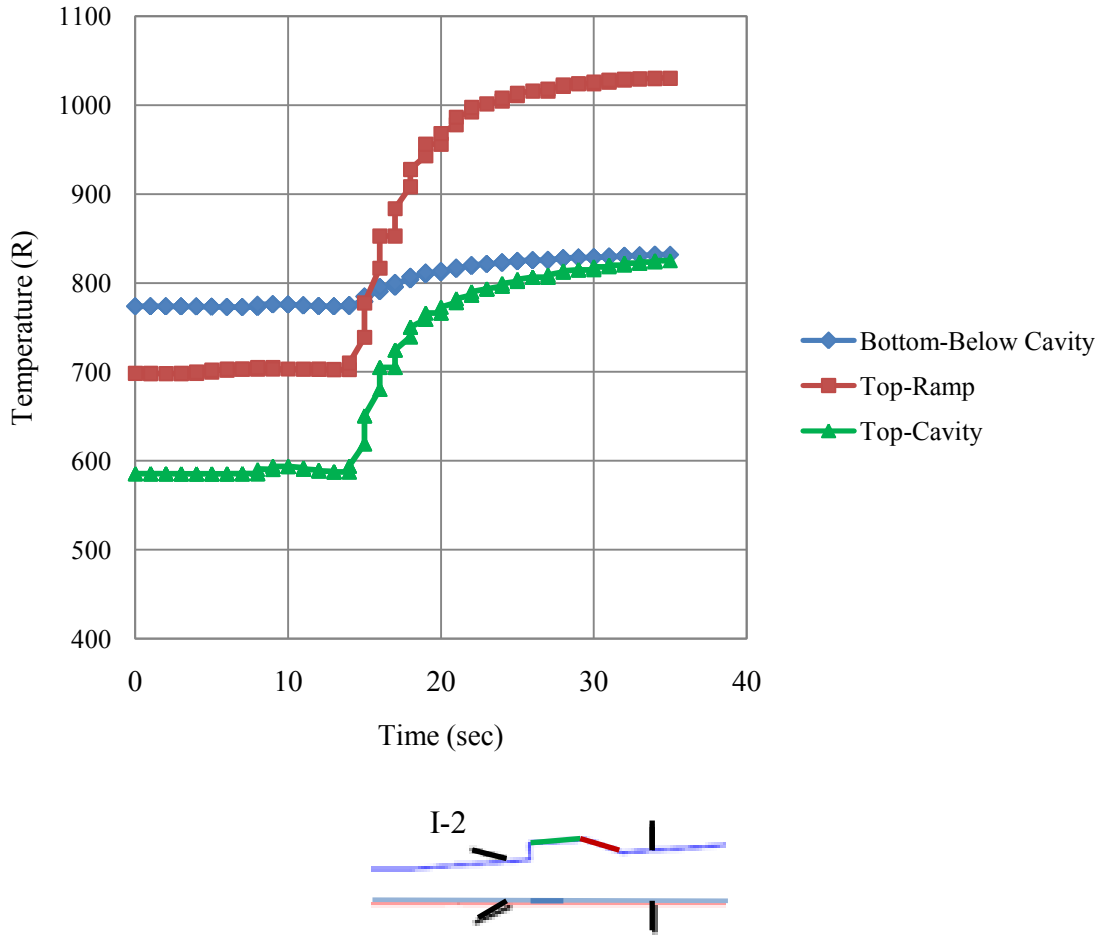

Figure 9: Cavity temperature profile and thermocouple locations

Three thermocouples were selected, including one in the top cavity, one on the top ramp, and one on the bottom wall directly below the cavity. This graph shows obvious differences in the starting temperatures of each of the thermocouple readings. In the first ten seconds of the run only air is flowing. Each of the thermocouples is expected to read a similar temperature. However, in this case there is a starting temperature difference of nearly 200 degrees Rankine. This large variance is due to the position of the thermocouples with respect to the wall and differences in water-cooling rates. If the thermocouple is not positioned in direct contact with the wall it will read a cooler temperature. Also, the water flow rates are not consistent throughout the rig. This means that one of the walls could be cooled at a faster rate than the other walls. While the temperature itself is important, in this study we are primarily concerned with the change in temperature over the run period. Therefore, the temperatures were normalized in order to depict a more accurate temperature increase over time. This technique allows the temperature trends to be accurately analyzed without the concern of uncertainties due to thermocouple placement or water-cooling flow rates. The normalization process was conducted by first finding the change in temperatures for each thermocouple over the specified time period. Each value was then divided by the thermocouple with the largest delta temperature, which was located on the ramp of the top side cavity. The normalized version of this same data is shown in Figure 10 and further discussed in chapter 4.

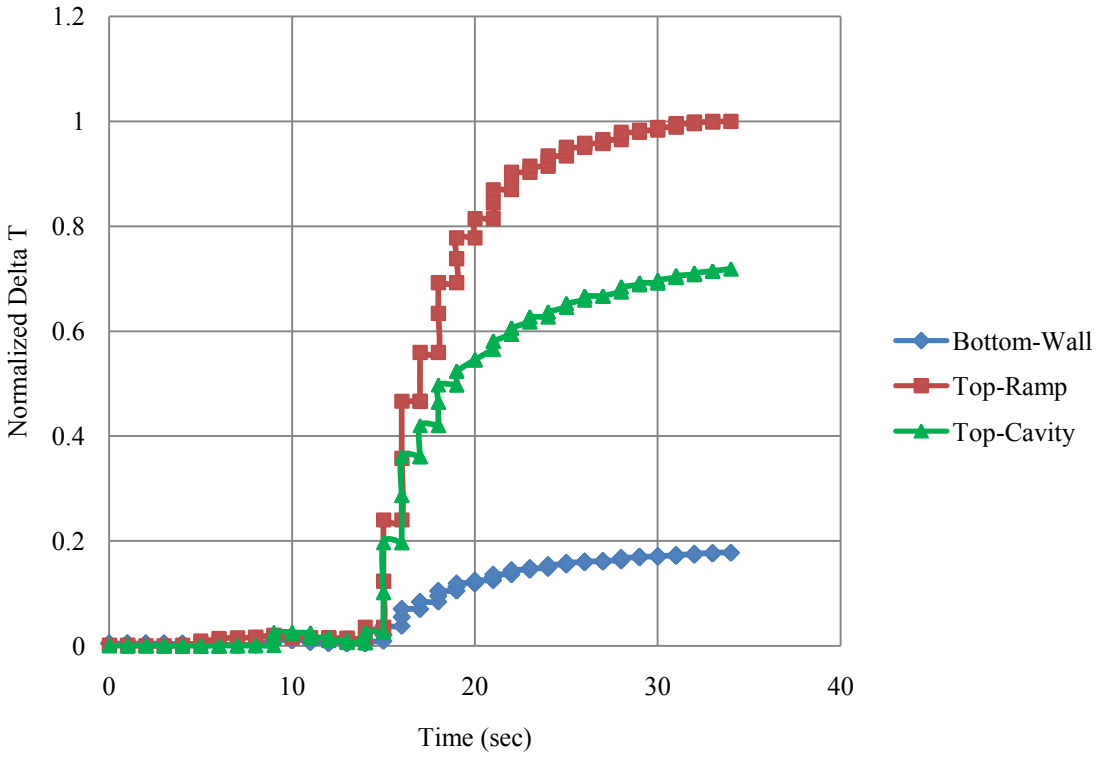

Figure 10: Normalized cavity temperatures

III.5 Uncertainty Analysis

Each of the calculated performance parameters has errors associated with conditional variations and systematic errors from the test facility. Total errors were calculated for the pressure readings, stream thrusts, and combustion efficiencies from one representative run. Standard error of the conditional variations with a 95% confidence interval was found using Equation 1.

$$Standard\ Error = 1.96\left(\frac{\sigma}{\sqrt{n}}\right) \quad (1)$$

An extensive uncertainty analysis of the systematic error has previously been conducted for the research rig by Smith, et al (13). The uncertainty calculation includes accuracy determination of the individual measurement devices, calibration standard accuracy, data-acquisition-system effects, individual sensor calibration, sensor measurements, influence coefficient determinations, equilibrium-code calculations, and performance variable determinations. Measurement uncertainty can be broken down into bias and precision components. The bias component, due to assignable causes (non-random), is the difference between the mean reading and the true value of the reading. The precision component, due to random non-assignable causes, is associated with the repeatability of the measurement and can be determined by taking repeated measurements. An example uncertainty associated with five measurements of a pressure transducer is shown in Figure 11.

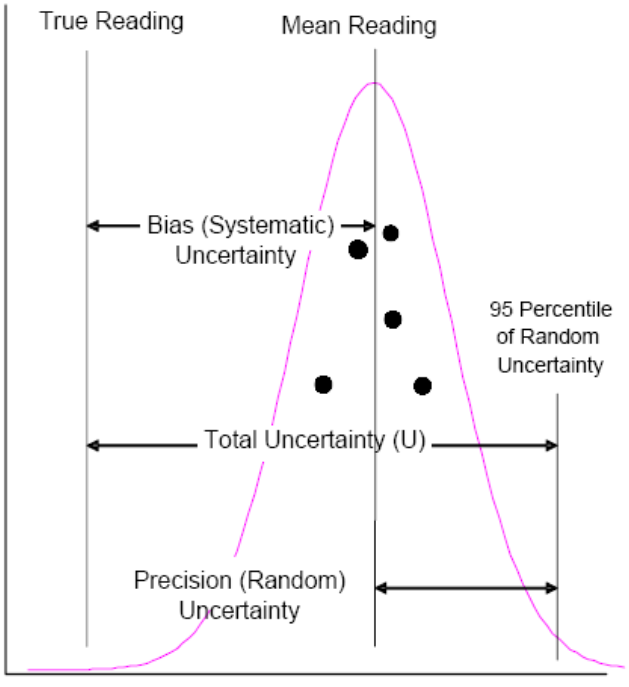

Figure 11: Measurement Uncertainty (13)

The precision uncertainty is the difference between the mean of the reading and a line that represents the 95th percentile of all measurements taken of a particular sample. The total uncertainty of a measurement is the combination of the bias component and the 95th percentile measurement of the precision component (13).

In this study, the stream thrust standard error was found to be 2.34%. The systematic uncertainty values for stream thrust total 1.23% (13). Geometric addition of these two uncertainties, shown in Equation 2, yields a total error of 2.64% for the stream thrust.

$$Total\ Error = \sqrt{(0.0234^2 + 0.0123^2)} = 0.0264 = 2.64\% \qquad (2)$$

This procedure was repeated for the combustion efficiency with a known systematic error of 4.73% (13). The standard error was 1.38% and the total error for efficiency was found to be 4.93%.

Finally, an uncertainty analysis was conducted for the measured pressures from run 329AR. A 95% confidence interval was used and found to be 3.50%. Uncertainty from the pressure system itself adds only 0.05% additional error (14). The total uncertainty for the pressure measurements is shown with error bars in Figure 14 in Chapter 4. All other runs are assumed to have similar error values.

IV Discussion and Results

IV.1 Equivalence Ratio

The seven cases chosen for direct comparison had total equivalence ratio set points of 0.6, 0.9 and 1.1. Cases 1, 4, 5, and 6 were set to $\phi = 0.6$, cases 2 and 7 were $\phi = 0.9$, and case 3 was $\phi = 1.1$. However, due to small changes in actual air and fuel flows, the equivalence ratios varied slightly from their set points. Due to these changes, the equivalence ratios between the single and dual cavity runs for each case were somewhat different as explained below. Figure 12 shows how closely the actual equivalence ratios compared.

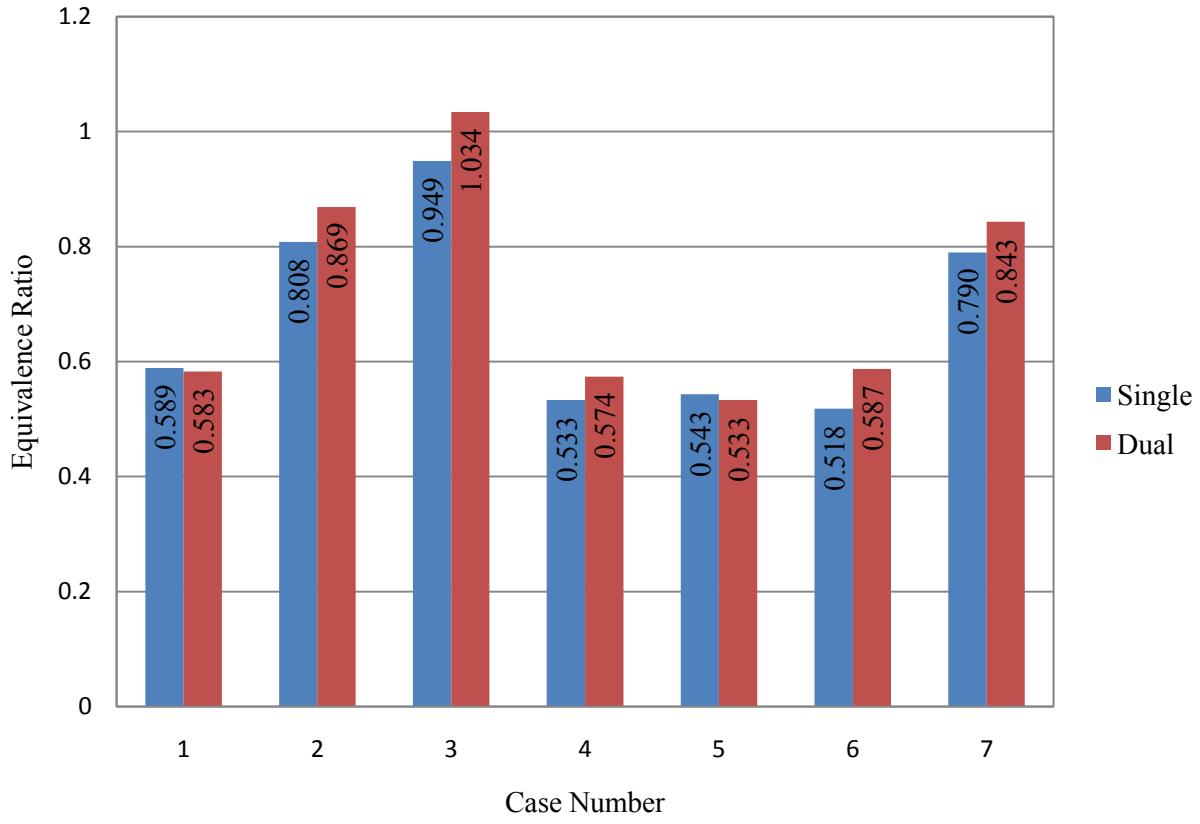

Figure 12: Total equivalence ratio

Case 1 had very similar conditions, with the single cavity having only a 0.006 higher ER. For comparison purposes, these two conditions are considered the same. Performance parameter comparisons, such as thrust and combustion efficiency, would need to take any ER differances greater than approximately 0.05 into consideration. While cases in this range are acceptable for direct comparison, small changes in performace could be caused by the increased or decreased ER. Cases 2, 3, 6 and 7 fall into this range. Cases 4 and 5 have less than 0.005 of a difference in their ER values, and while any significant change in performace due to this small fueling difference is unlikely, it is still necesary to consider when analyzing the results.

IV.2 Pressure Profiles

The first parameter considered for performance and operability was the axial pressure distribution. In order to make the analysis process less complex and more efficient, it was decided to only use the pressure taps from one wall of the flow path. However, this would only work if the pressures from all walls were consistent. In order to show consistency, one case was chosen and the axial pressure distribution was plotted for all walls. The three walls with significant instrumentation are plotted in Figure 13. The top wall of the flow path is shown in black in order to correlate high pressure regions to physical locations.

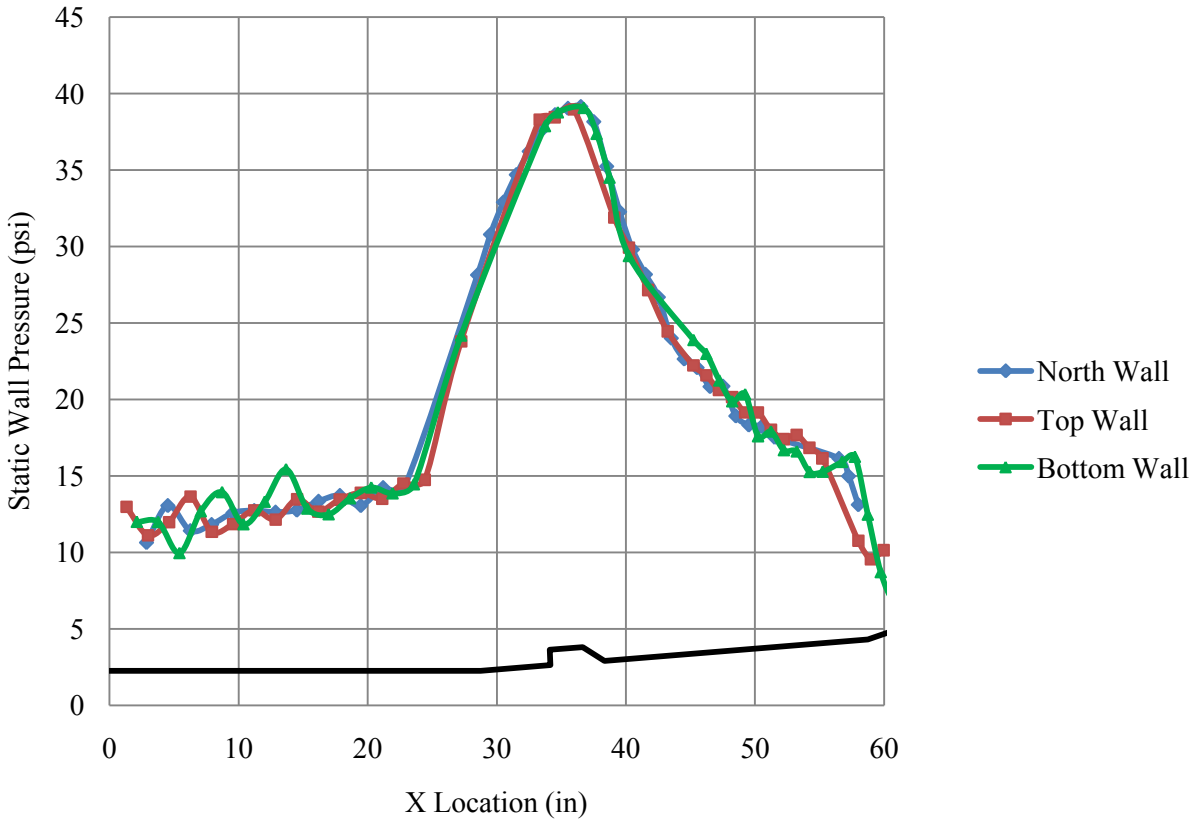

Figure 13: Wall pressure comparison

Each point is an average of the pressure tap reading over the time of steady state combustion, typically eight to ten seconds, or 40 to 50 readings. As shown above, the pressures from the north side wall, the top wall, and the bottom wall all align fairly closely. They each have very similar peak pressures and show the same pressure rise and fall throughout the flow path. The small variance in the top and bottom wall readings inside the isolator is assumed to be due to a reflecting shock. From this analysis, using only the north wall provides an accurate depiction of the physics occurring on all sides of the flow path. The north wall was chosen due to the greater number of pressure taps as compared to the other walls. The north wall also has the same taps regardless of which

flow path (single or dual cavity) is being used. When the bottom side cavity is installed, the pressure taps on the bottom wall will be at different locations, but the north wall tap locations will not change.

Figure 14 shows the axial pressure data from the single cavity run of case 5. The red line is the pressure profile when only air is flowing and no fuel is being injected. The blue line shows the pressure during the period of steady state combustion.

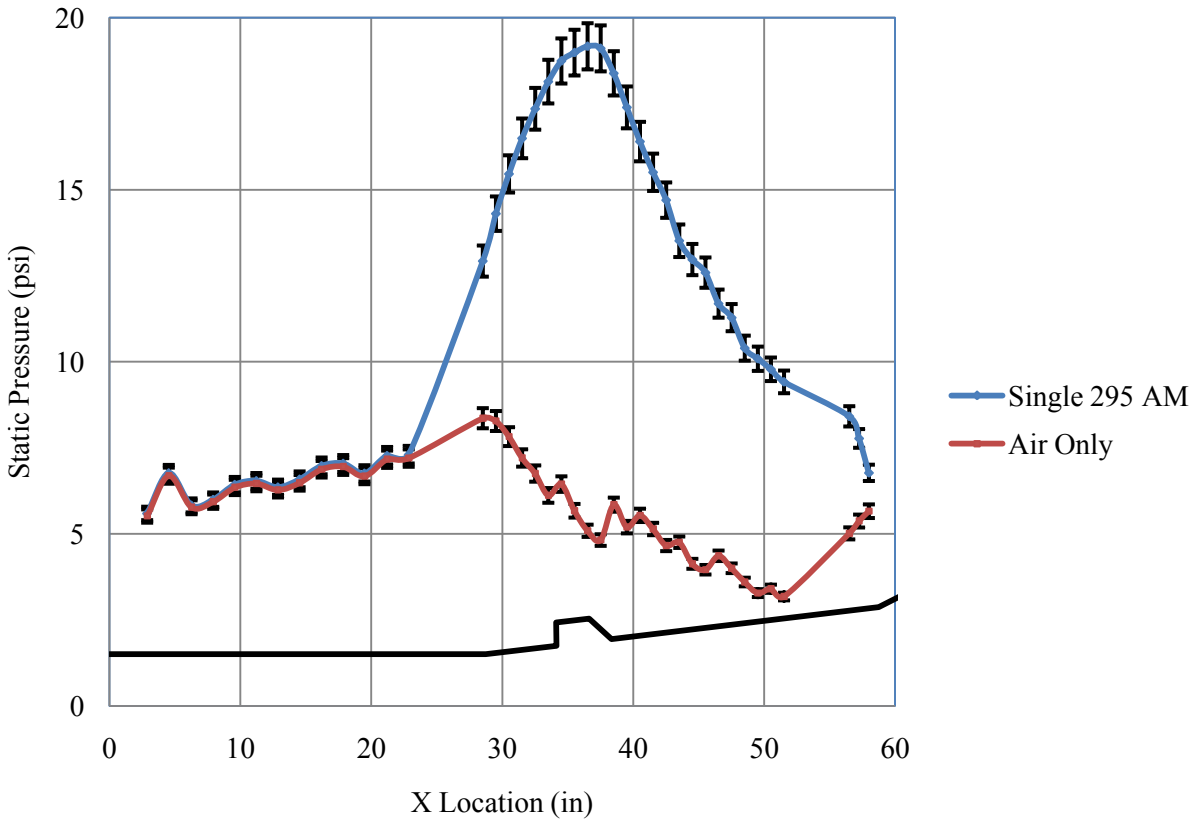

Figure 14: Pressure versus axial position with error bars

During combustion, the drastic increase in pressure occurs at the beginning of the shock train. If the shock train moves too far upstream in the isolator it would cause an unstart. The unstart would be seen on the pressure profile graph as a separation between

the two lines occurring within the first two pressure points at x = 2.9 and x = 5.4 inches. That is, the tare (air only) and combustion profiles would be separated. Here, tare and combustion are identical until x = 24. If only one, or none, of the first two points overlap, the run would be considered an unstart. This will be a primary method of characterizing the operability of the flow path. These pressure profiles help to explain what is occurring throughout the flow path. The large pressure near the flame holder is due to significant heat addition in that area. The increased pressure from the divergent wall starting at approximately x = 40 yields significant thrust due to the change in area. The tare profile shows separation of the flow near the truncated nozzle. The flow is detaching from the wall as it hits the increased area at the entrance to the truncated nozzle causing the pressure to rise quickly. The combustion flow at this point does not separate due to the increased pressure from the combustion process. Figure 14 also shows the 3.5% uncertainty due to systematic and random errors. The variations in the air only run throughout the combustor are not due to errors. These fluctuations are caused by a shock wave off the back of the cavity and an expansion wave off the front of the cavity.

Case 1 compares the single cavity run 295AB and the dual cavity run 329AM shown in Figure 15. Each of these runs was conducted with the M = 2.2 facility nozzle and an equivalence ratio of approximately 0.58. The fuel was injected from I-2 on the top side of the flow path, upstream of the cavity, in both cases. The dual cavity run shows a slightly more upstream shock position. It also has an increased peak pressure and slightly higher exit pressure. An increase in pressure such as this is usually due to an increase in heat release resulting in better performance.

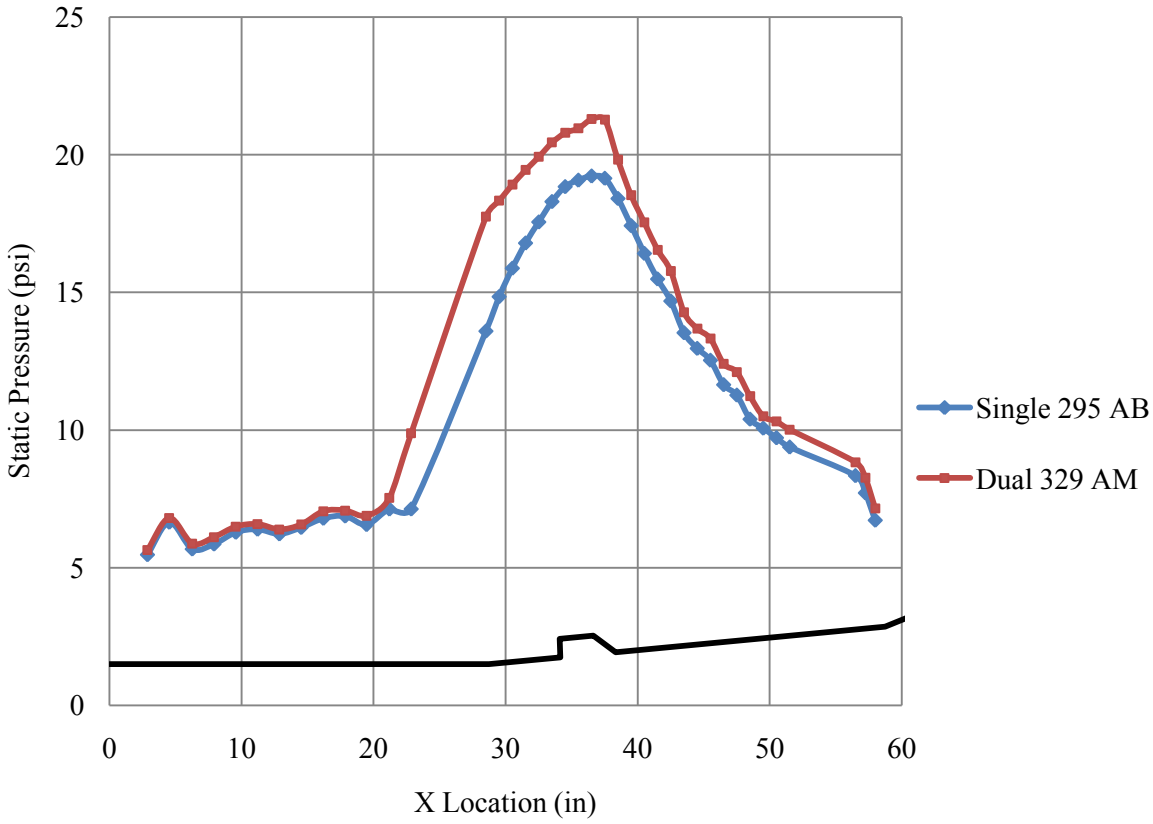

Figure 15: Case 1 pressure profile

Figure 16 shows the pressure profiles for case 2. Runs 295AK and 329AN represent the same flight conditions as case 1, but had equivalence ratio set points of 0.9. The actual run ERs were slightly lower at 0.808 for the single cavity run and 0.869 for the dual cavity run, both with I-2 only fuel injection.

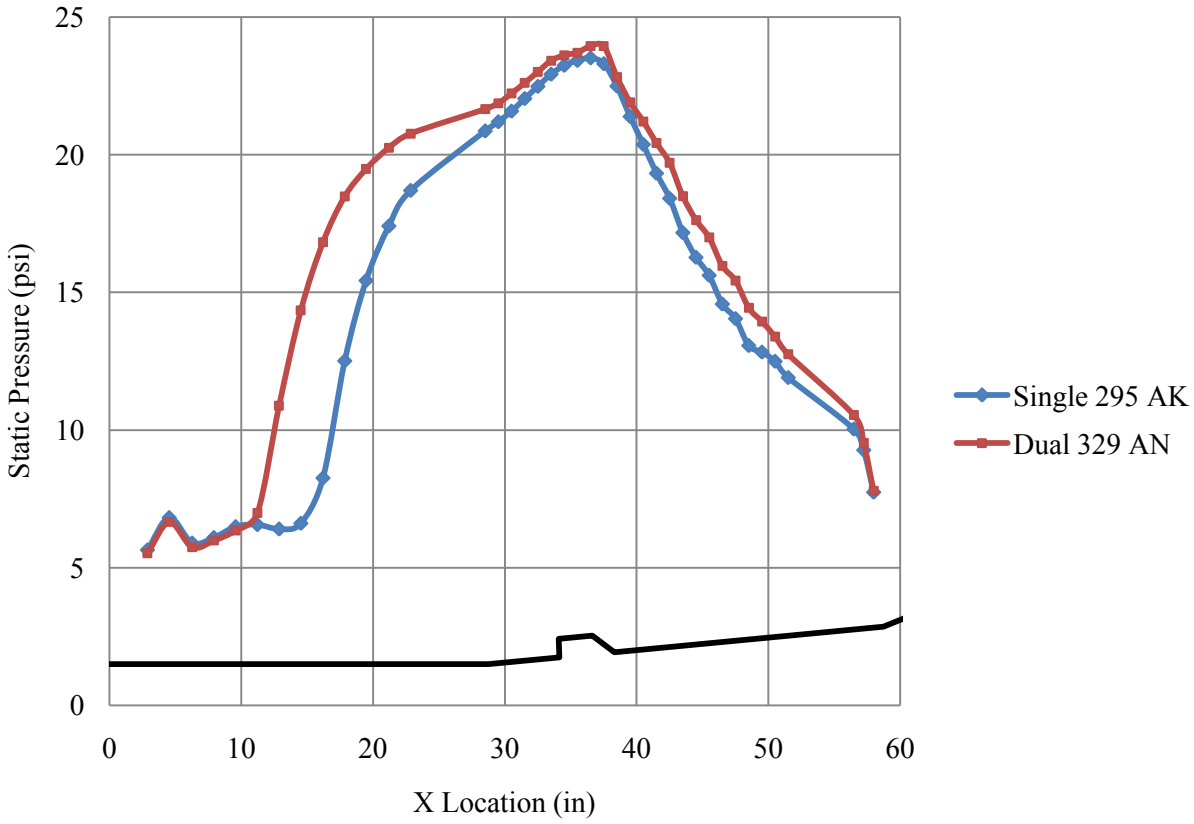

Figure 16: Case 2 pressure profile

The graph shows the same trends as for case 1, but with an upstream shock location further forward than in case 1. Each of these runs have the first five pressure taps overlapping, indicating neither case is an unstart. However, the operabilty margin, or the isolator length remaining before unstart, with this equivalence ratio is reduced from case 1 where $\phi = 0.6$. The dual cavity again shows a slightly higher peak pressure as well. In this case, the equivalance ratios are slightly different, which could account for a small portion of the dual cavity having a shock position further upstream and higher peak pressure. However, there is a substantial difference in the shock position of nearly four inches. This is not caused purely from the difference in fueling. Therefore, the dual cavity is providing some additional performance capabilities.

The equivalence ratios for case 3 were set even higher, at ϕ = 1.1. The actual ERs were 0.949 for the single cavity and 1.034 for the dual cavity flow path. Figure 17 shows the dual cavity run was an unstart. The first two points are separated from their position in the single cavity case. When an unstart occurs, there is no guarentee the test conditions were ever met. The unstart also provides information on the operability of the dual cavity. Thus far, with I-2 injection, the dual cavity will operate at equivalence ratios between approximately 0.58 and 0.87, but not up to 1.03. This could provide negative consequences as equivalence ratios above 1.0 are often neccessary for periods of rapid acceleration.

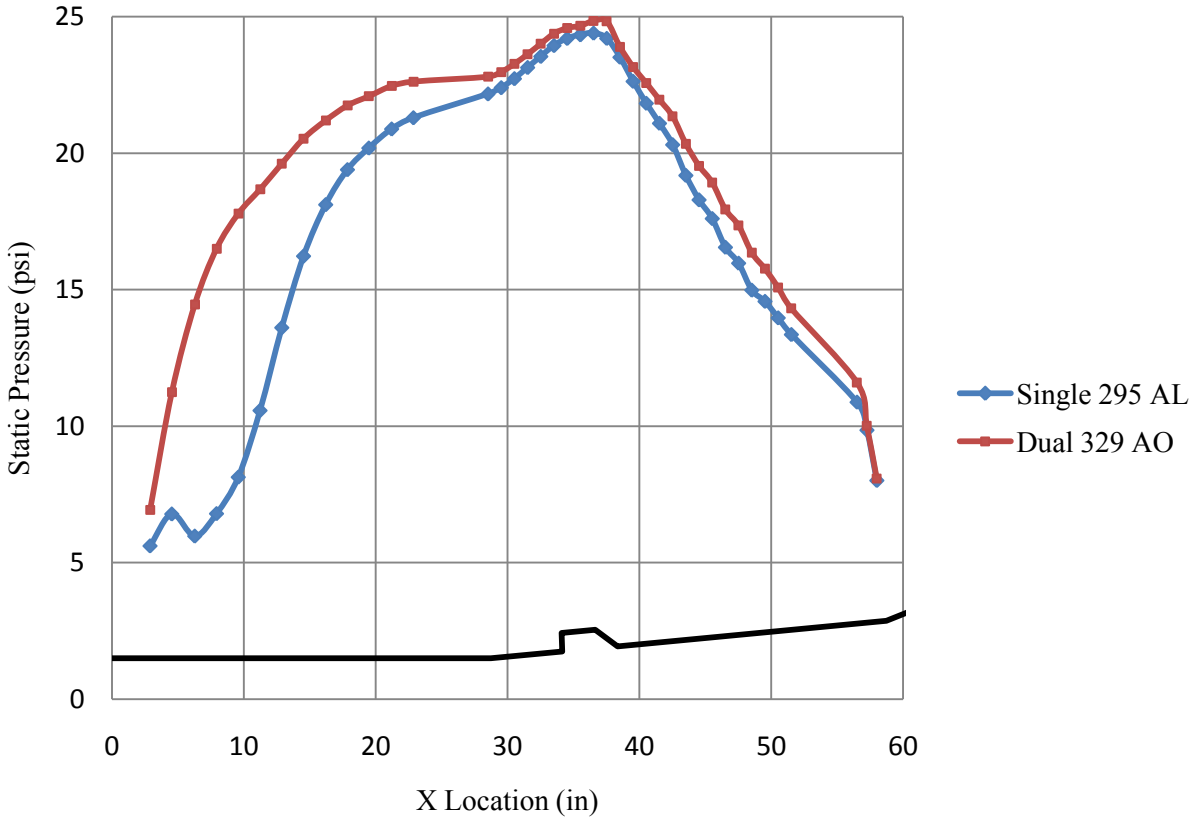

Figure 17: Case 3 pressure profile

Case 4 results are shown below in Figure 18. In this case, the single cavity was fueled from I-2 only while the dual cavity utilized both I-2 and I-4 injection sites. The single cavity run had an equivalence ratio of 0.533. The dual cavity had an I-2 ER of 0.293 and an I-4 ER of 0.234 for a total of 0.527. The absolute fuel flow into the combustor varied slightly between the single and dual cavity runs with rates of 0.069 and 0.073 lb_m/sec, respectively. It is obvious from the pressure profile graph that the dual cavity flow path provides a much greater pressure rise than the single cavity. In the dual cavity run, both top and bottom flame holders are actively involved. This results in significant heat release from both causing a large overall pressure rise. The shock position is also farther upstream, but not to the point of unstart.

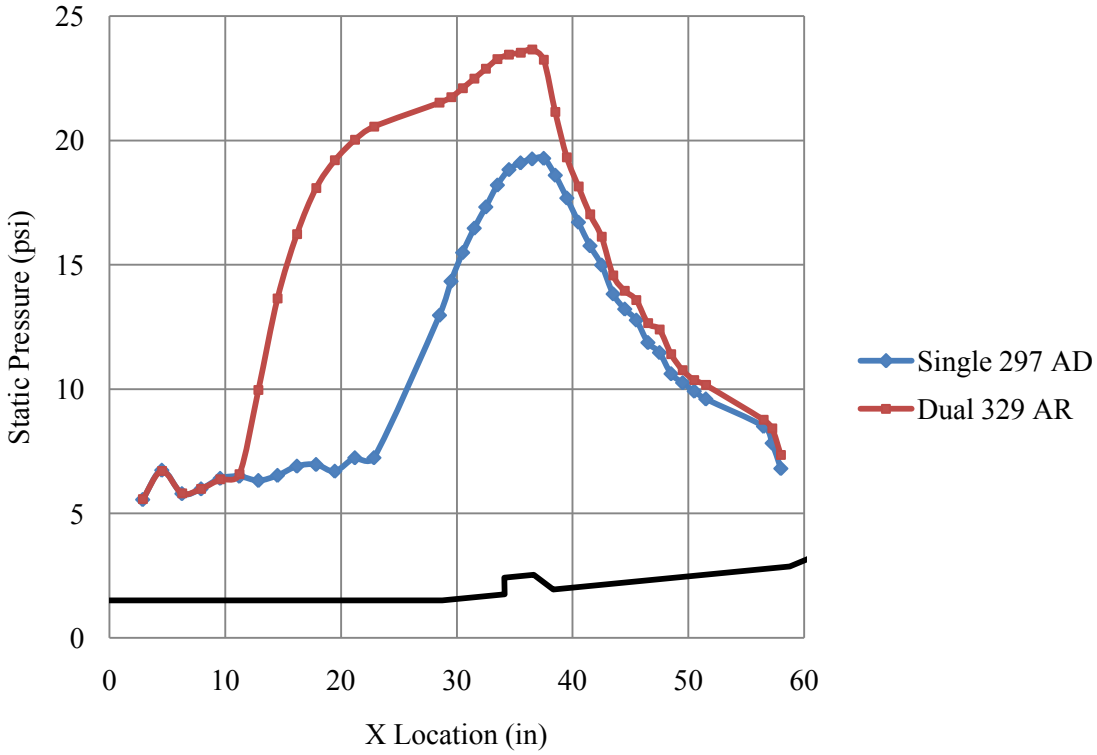

Figure 18: Case 4 pressure profile

Figure 19 shows the pressure profiles for runs 295AM and 323AN from case 5 along with the two runs from case 4. Case 5 is a repeat of the flight conditions and fueling schemes from case 4. The runs were taken from different nights in order to test the repeatability of the results. The single cavity run had an ER of 0.543 and the dual cavity run had a total equivalence ratio of 0.520. The pressure profiles show the same results as case 4. The single cavity runs overlap perfectly and the dual cavity runs are very close. Both of the dual cavity flow path runs have a shock train position farther upstream than the single cavity runs. They also have a much higher peak pressure indicating greater heat release.

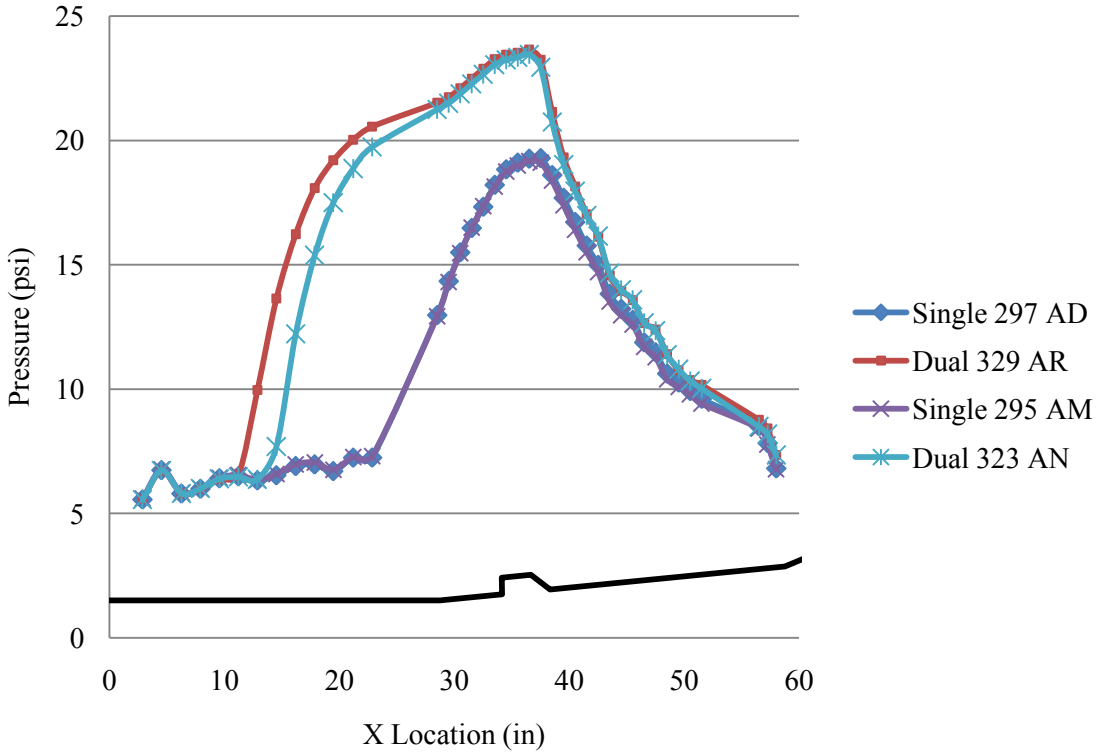

Figure 19: Cases 4 and 5 pressure profiles

Case 6 is shown in Figure 20. This case was conducted using the M = 2.2 facility nozzle, but with higher input temperatures and pressures. These conditions correspond to higher flight Mach and dynamic pressure values. The fueling is similar to cases 4 and 5 with the single cavity using only I-2 injection and the dual cavity run having fuel split between I-2 and I-4. The single cavity run had a slightly lower equivalence ratio at 0.518 than the dual cavity run with a total equivalence ratio of 0.571. The dual cavity run again shows a higher peak pressure and a shock position significantly upstream in the isolator. It has higher pressures downstream of the cavity as well.

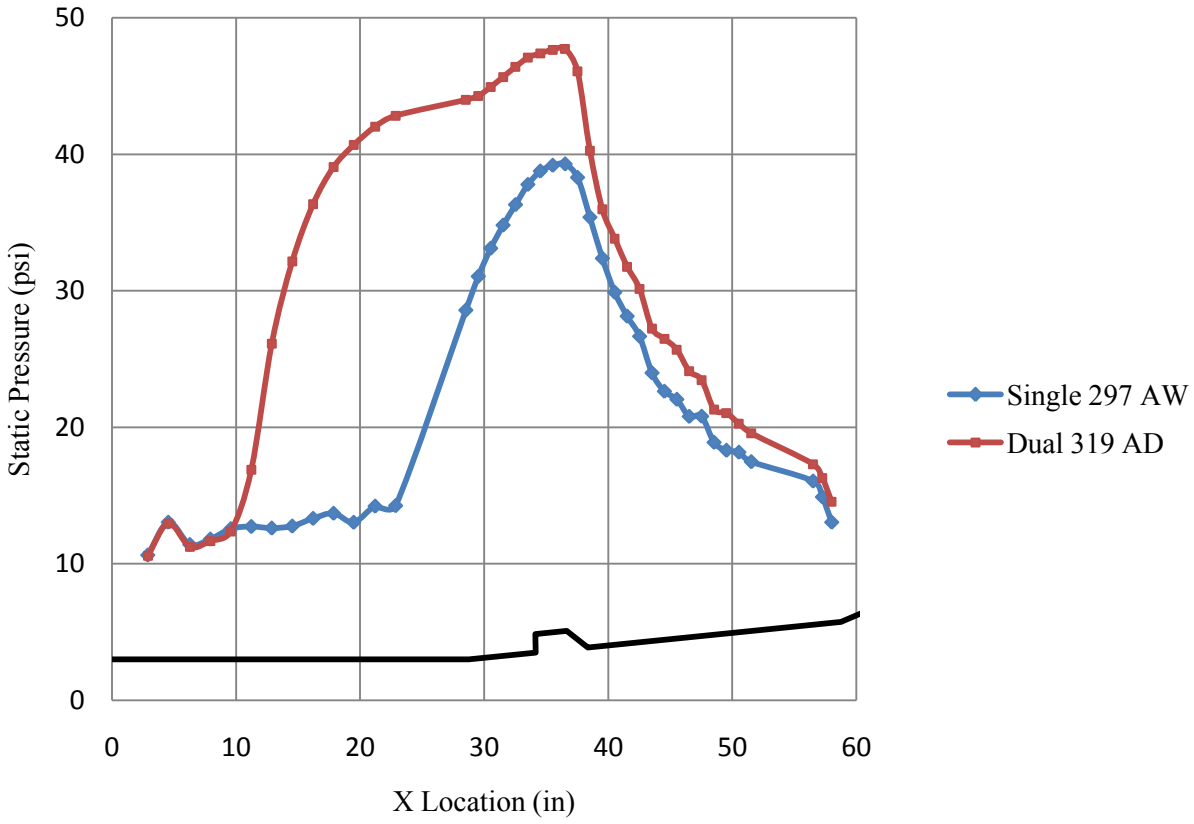

Figure 20: Case 6 pressure profile

The final pressure profile comparison is for case 7 and is shown in Figure 21 below. This case utilizes both upstream and downstream fueling. The single cavity run, 297AD, has fuel split between I-2 and I-5 and has a total equivalence ratio of 0.78. The dual cavity run uses I-2 and I-4 upstream and I-5 and I-7 downstream of the cavities. The dual run, 319AJ, has a total ER of 0.836. This case shows the greatest difference in shock position and peak pressures between the two runs of any of the cases. The fueling scheme from the dual cavity run provides a significant advantage in pressure increase over the single cavity. However, while the dual cavity run is not considered an unstart, it is very close. Any increase in fueling would likely push the shock upstream and cause it to unstart.

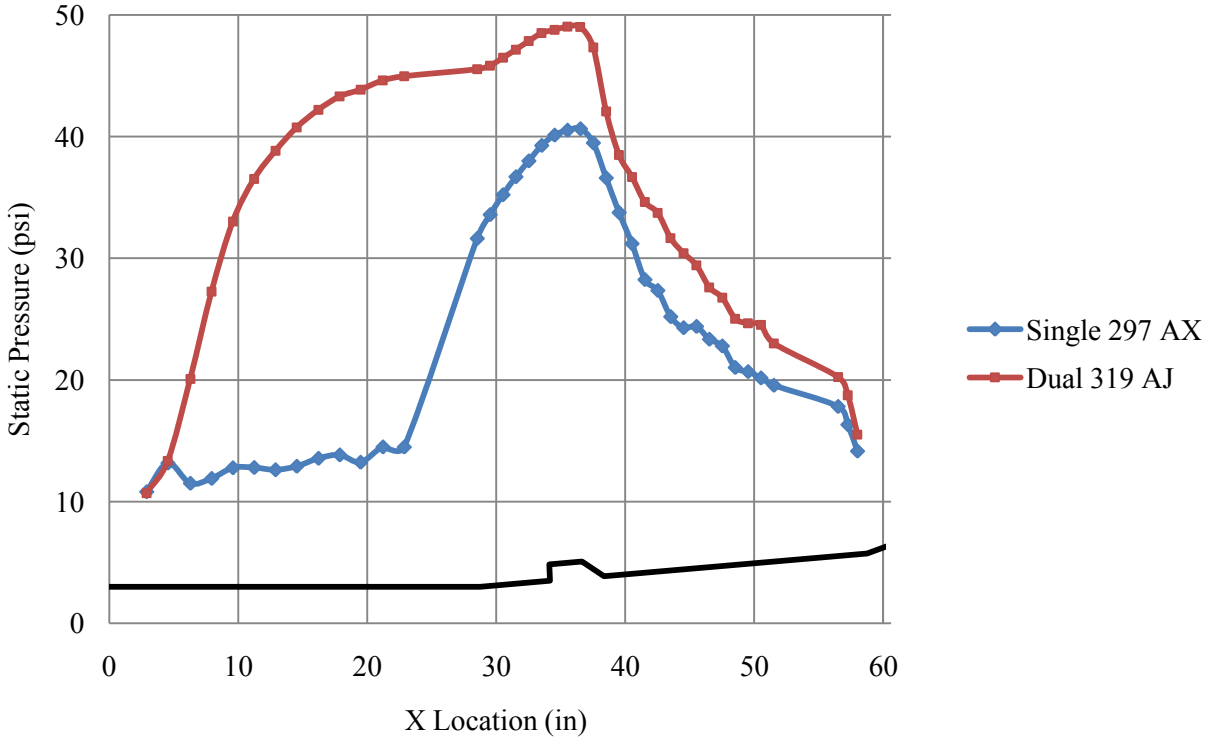

Figure 21: Case 7 pressure profile

IV.3 Peak Pressure Ratio

Figure 22 below shows the peak pressure ratios for each run. The peak pressure ratio is determined by dividing the peak pressure from the flow path by the lowest pressure. The highest pressure is located in the cavity, while the lowest pressure is always from the first pressure tap in the isolator.

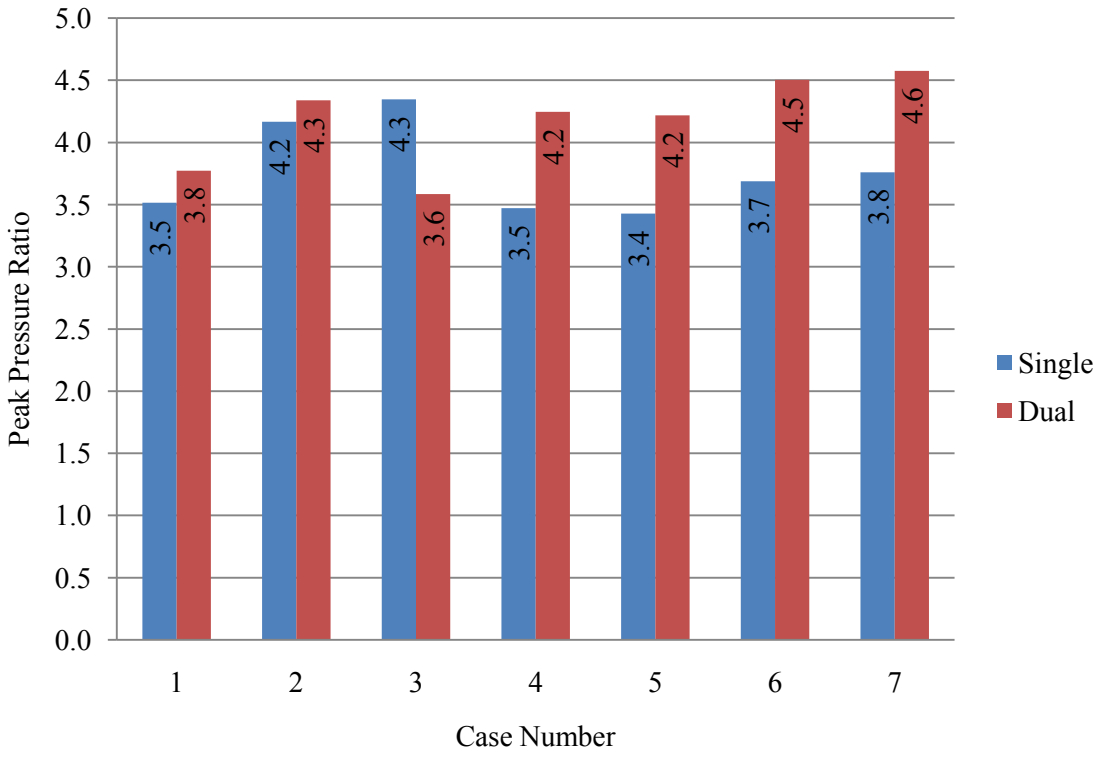

Figure 22: Peak pressure ratios

Each case shows a higher peak pressure ratio for the dual cavity flow path, except for case 3. This is likely due to the unstart and may be an unreliable value. Cases 1 and 2 have only an 8.6% and 2.4% increase, respectively. However, cases 4-7 that have fueling from both the top and bottom sides show a significant increase of 20% or more. This

increase in peak pressure ratio is due to a greater heat release, suggesting the dual cavity is providing better combustion.

IV.4 Combustor Exit Pressure Ratio

The combustor exit pressure ratio is another way to characterize performance changes relative to the cavity configurations. It is found by taking the pressure reading from the last pressure tap in the combustor and dividing it by the lowest pressure found at the beginning of the isolator. The combustor exit pressure ratios are shown in Figure 23.

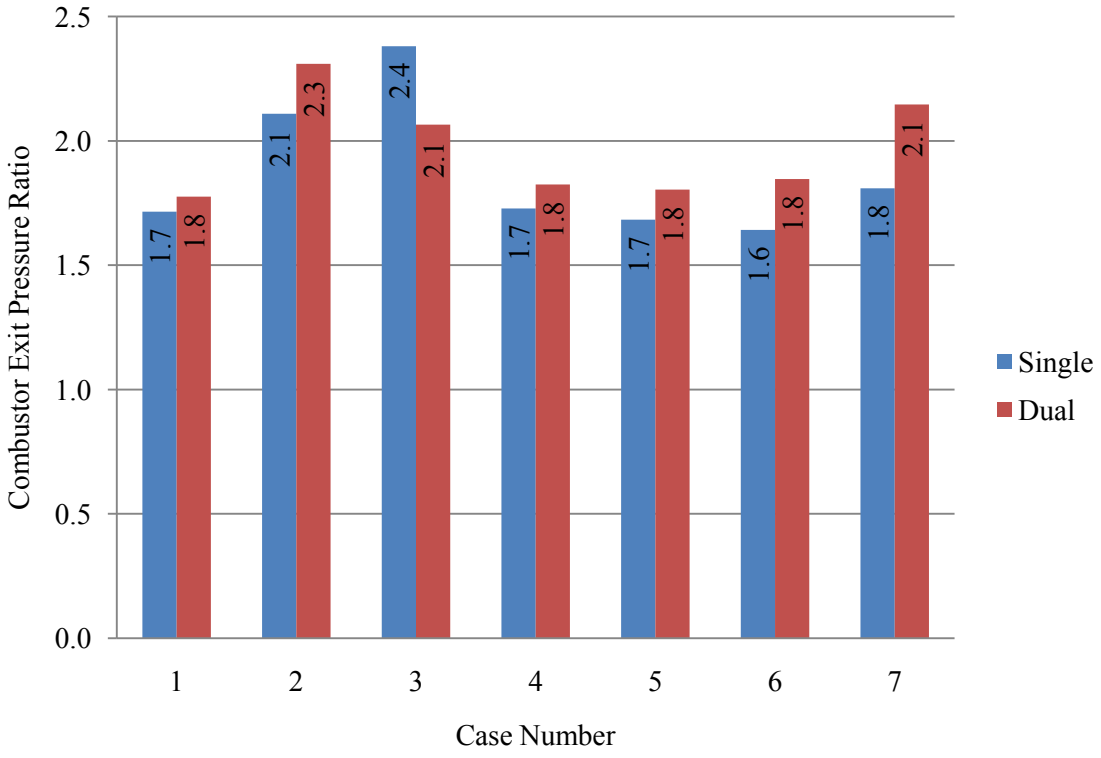

Figure 23: Combustor exit pressure ratios

Each case shows a slightly higher ratio for the dual cavity runs. The only exception is case 3, due to the unstart. There is a difference of 5-17% for each case. For the same combustor geometry, isolator inlet conditions, and fuel flow rate, higher exit pressures mean greater heat release. Therefore, the increase in exit pressure is further evidence that the dual cavity may be providing better performance than the single cavity flow path.

IV.5 Load Cell Force and Stream Thrust

Another way of determining performance is by comparing load cell force and stream thrust. Figure 24 shows the load cell force for each run.

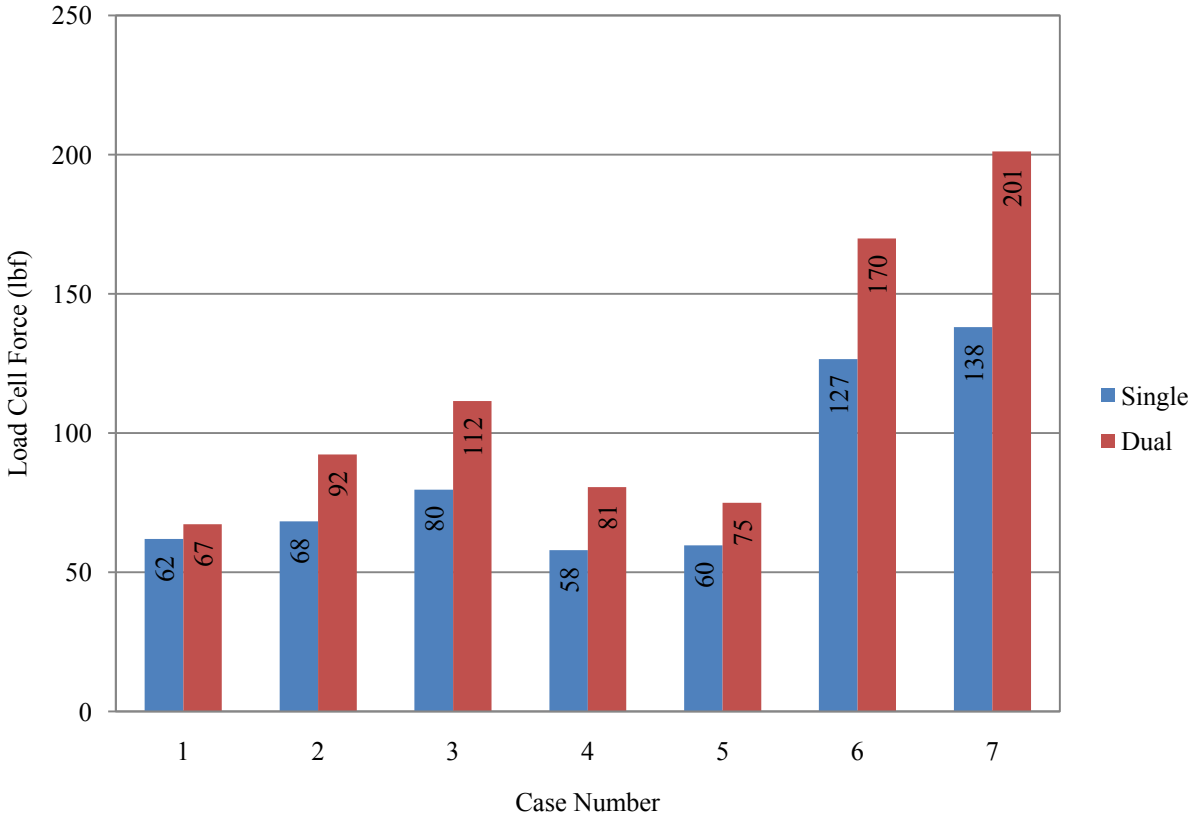

Figure 24: Load cell force comparison

These values are the average of the two load cell forces on the rig. Each case shows a significant increase when using the dual cavity flow path. The increase ranges from approximately 8% to 46%. The smaller values are for cases with lower equivalence ratios, as expected. At higher equivalence ratios, and when fuel is injected from both top and bottom sides, the load cell force dramatically increases. These force increases are reasonable and expected with the changes in fueling.

While the load cell force gives an approximation of the forces on the rig, the better parameter to determine performance is stream thrust, which accounts for the losses subtracted from the load cell forces. The stream thrust is found using the momentum equation for control volume analysis:

$$ST = F + P_{amb}\,A_E + (P_{amb} - P_{base})A_{base} \tag{3}$$

where F is the load cell force, P_{amb} is the ambient pressure, A_E is the exit area, and P_{base} is the average of the twelve base pressures from the end of the truncated nozzle. The exit area had a value of 17.132 in^2 and the base area was 23.39 in^2. The stream thrust values are shown in Figure 25.

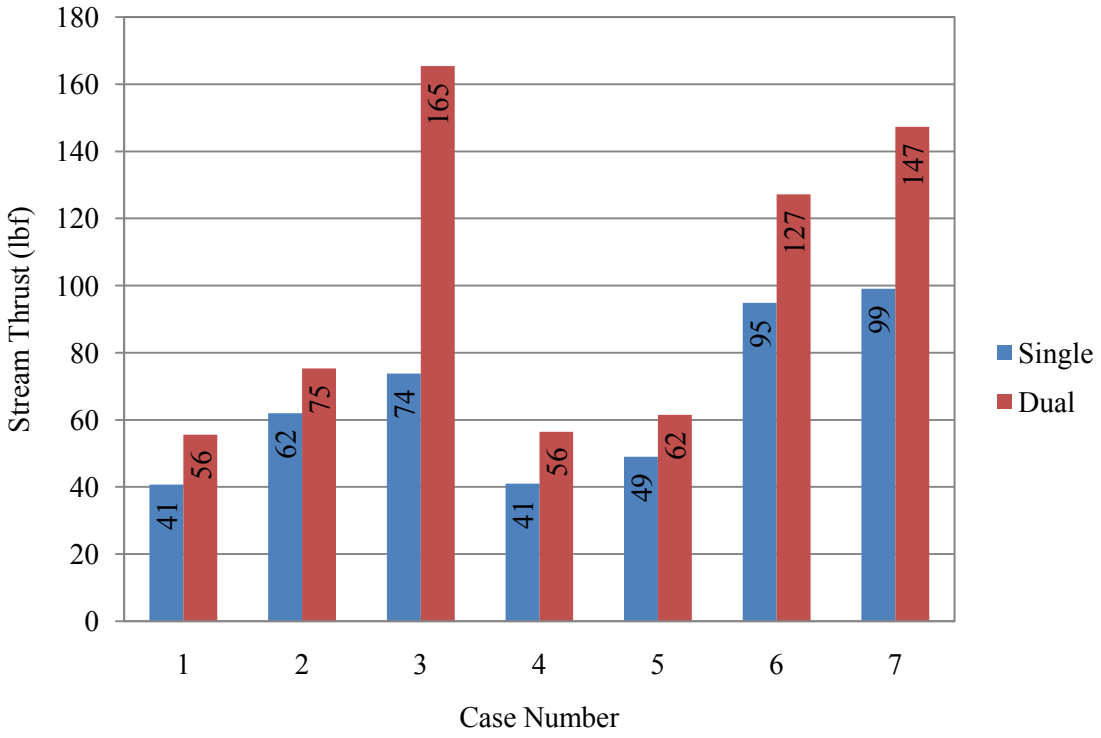

Figure 25: Stream thrust comparison

Each case has a stream thrust significantly higher for the dual cavity than for the single cavity. The stream thrust for case 3 has an extremely high value due to the unstart and is not an accurate reflection of the true run conditions. For all other cases, the dual cavity has an average of over 34% higher stream thrust with the greatest difference in cases 6 and 7 where higher flight Mach and dynamic pressure conditions are used with fueling from both top and bottom side injectors.

To further verify these results, the stream thrust values were normalized to account for differences in the fuel flow rate between the single and dual cavity runs for each case. The normalization was accomplished by dividing the stream thrust by the total fuel mass flow rate. These normalized stream thrust values are found in Figure 26.

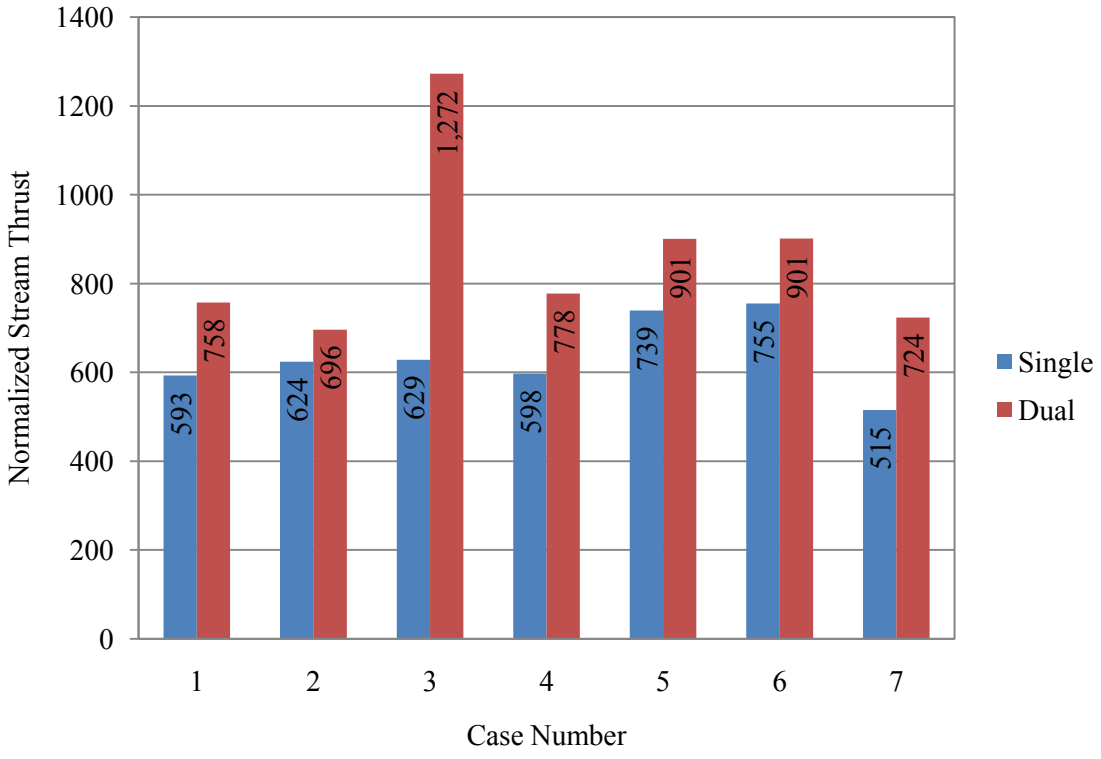

Figure 26: Normalized stream thrust comparison

The normalized stream thrust values show the same trend as the original stream thrust comparison. The high value for the dual cavity run of case 3 is again due to the unstart. Each dual cavity run has a higher value than the single cavity. Therefore, these differences in stream thrust are due to increased performance, not differences in fuel flow rates. The increase of stream thrust with the dual cavity is further evidence that the effect of adding the additional flame holder is to provide better performance.

IV.6 Shock Position

Figure 27 shows how the position of the shock train relates to the total equivalence ratio. This is the primary determinant of operability. The position of the shock train is determined to be the first pressure tap where the ratio of its value divided by the tare value at the same location is equal to or greater than 1.1.

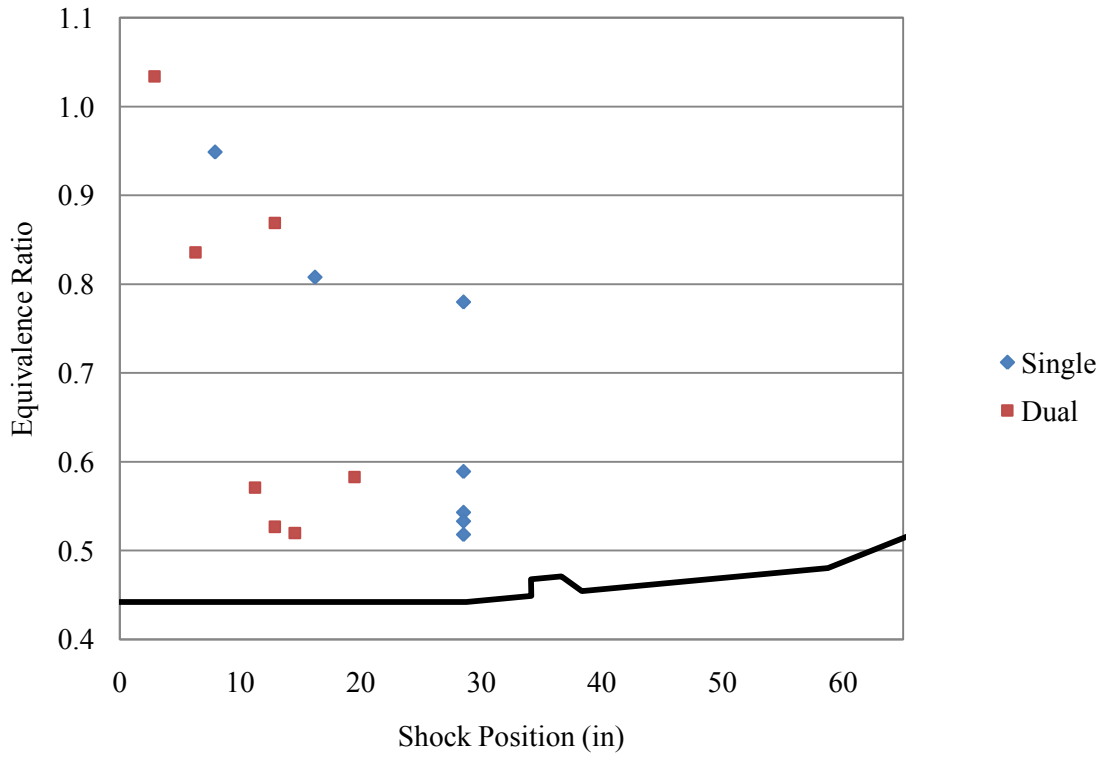

Figure 27: Shock position versus total equivalence ratio

Each run with the dual cavity configuration has a shock position farther upstream in the isolator than the single cavity flow path. The graph shows the dual cavity has a smaller range of operability and is more likely to unstart as the equivalence ratio is increased. The single cavity shock position also moves upstream as the equivalence ratio

increases, but it does not come as close to unstarting as the dual cavity flow path does. The single cavity points shown at 28 inches actually represent a shock position anywhere between 25 and 28 inches. This area is the connection between the isolator and the combustor and has no instrumentation.

IV.7 Combustion Efficiency

The combustion efficiency is another parameter for determining the performance of a combustor by measuring the percentage of injected fuel that is being burned. For this research, a previously developed in-house code called QPERF was used to determine the efficiencies from the captured data. QPERF solves the one-dimensional equations shown below for the control volume in Figure 28. It uses the measurements of the reactant mass flow rates, load cell force, heat loss, base pressure, exit pressure and ambient pressure (13). QPERF also uses a chemical equilibrium package with values for the molecular weight, static temperature, and the mass fraction of frozen or unburned fuel. The equations below are solved simultaneously.

$$\rho_5 U_5 A_5 = W_A + W_F = W_5 \tag{4}$$

$$W_5 U_5 + P_5 A_5 = ST_5 = F + P_{amb} A_5 + (P_{amb} - P_{base}) A_{base} \tag{5}$$

$$W_5 (H_5 + 0.5 U_5^2) = W_A (H_A + 0.5 U_A^2) + W_F (H_F + 0.5 U_F^2) - Q \tag{6}$$

$$U_5 = \left(\frac{ST-PA}{W}\right)_5 \tag{7}$$

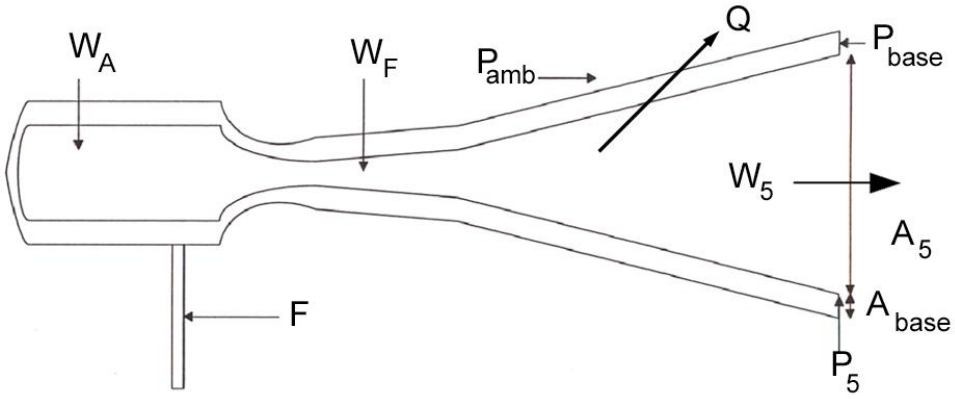

Figure 28: QPERF control volume

The reactant enthalpies are determined from the measured reactant temperatures. This leaves four remaining unknowns: exit density (ρ_5), exit enthalpy (H_5), exit velocity (U_5) and mass fraction of unburned fuel (Y_F). Equation 5 then yields the relationship for U_5 in Equation 7. This expression is then substituted into Equations 4 and 5 to yield ρ_5 and H_5, respectively. An initial value of Y_F is selected and fed into a chemical equilibrium package using the known exit pressure and enthalpy to yield the temperature and molecular weight of the mixture. The exit density is then found from the equation of state (Equation 8).

$$\rho_5 = \frac{P_5 * MW}{R_U * T} \tag{8}$$

Y_F is varied using a Newtonian iteration until the density from Equation 8 matches Equation 4 within the prescribed convergence criteria. Once Y_F is known, the total temperature is computed using the equilibrium code. Repeating the equilibrium calculation and setting Y_F to 1.0×10^{-6} yields the ideal total temperature (15). The total temperature at the facility nozzle exit is found by performing another equilibrium calculation of the combustion heater flow assuming all of the combustion heater fuel is consumed. Two measures of combustor efficiency are computed using either the mass fraction of frozen fuel (Equations 9 and 10) or the combustor temperature rise (Equation 11)(13).

$$\eta_{c,YF} = 1 - Y_F, \phi \leq 1 \tag{9}$$

$$\eta_{c,YF} = 1 - Y_F \phi, \phi > 1 \tag{10}$$

$$\eta_{c,\Delta T} = \frac{T_{T5} - T_{T4}}{T_{T5,ideal} - T_{T4}} \tag{11}$$

Both efficiencies were calculated in this study and were found to be very similar with the frozen fuel efficiency being slightly higher in each run. All values presented here are based on the mass fraction of frozen fuel (Equations 9 and 10). The combustion efficiency values are shown in Figure 29 along with the equivalence ratios for each run.

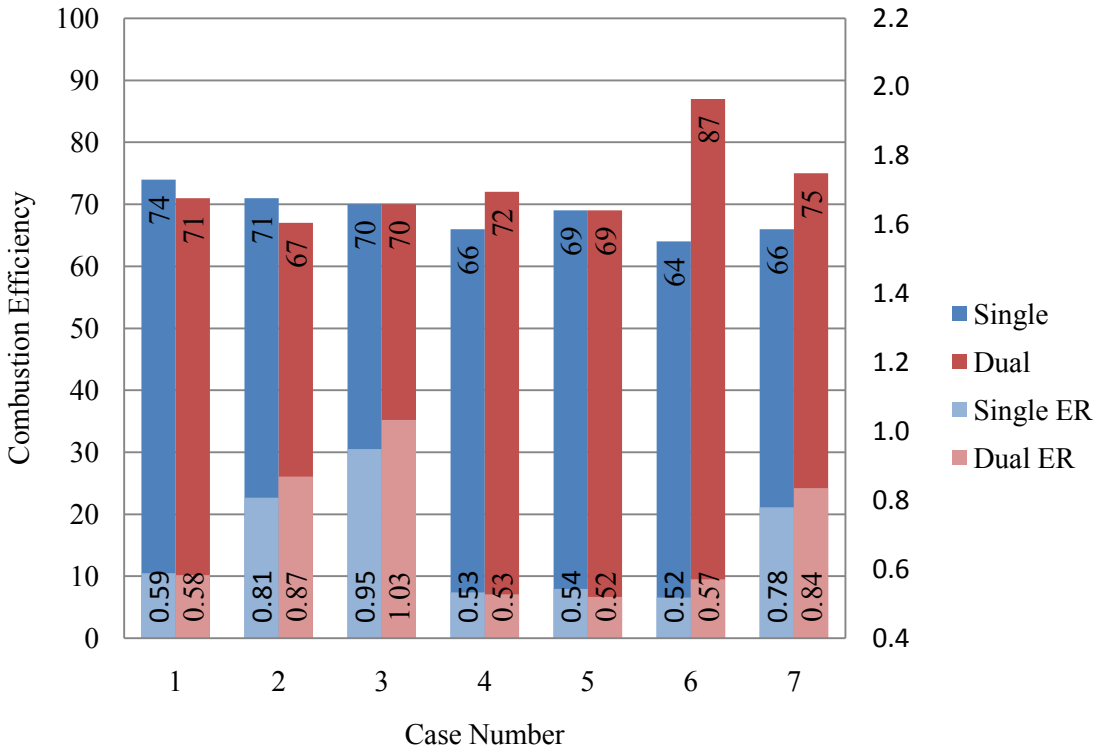

Figure 29: Combustion efficiencies based on the mass fraction of frozen fuel

Unlike the stream thrust and pressure profiles, it is difficult to find a trend in the combustion efficiency. The dual cavity does not show an increased efficiency for every case as would be expected from the trends in pressure and stream thrust. The calculated combustion efficiency uncertainty is 4.93%. Therefore, the single and dual cavity flow path runs in cases 1, 2, and 5 could have nearly the same efficiencies. Cases 1 and 2 may have similar efficiencies because only the I-2 injector is used. Cases 4, 6, and 7 do show a significant increase in efficiency for the dual cavity. However, after considering the performance parameters previously examined, the combustion efficiencies for all of the dual cavity runs would be expected to be larger than those of the single cavity flow paths.

The code used in these combustion calculations has not been fully verified for use in Research Cell 18. There are many inputs to the code that could be causing errors in the calculations. These items need to be verified before more dependable results can be obtained. Several possible errors are further discussed in Chapter 5.

Due to the possible uncertainties in the QPERF code, and the discontinuity between the combustion efficiencies and the other performance parameters, the efficiency values obtained are not considered reliable in this study. Further work and verification of the QPERF code would be beneficial in providing more accurate and consistent combustion efficiencies.

IV.8 Cavity Temperature

The stream thrust and pressure profiles suggest the addition of the dual cavity is somehow aiding in combustion. Cavity temperatures for three separate runs were studied to determine what may be causing this increase in performance. Figure 30 shows the normalized temperatures from three cavity thermocouples for the single cavity run in case 5. This figure was previously shown as Figure 10 in chapter three along with the normalization process, but is repeated here for convenience.

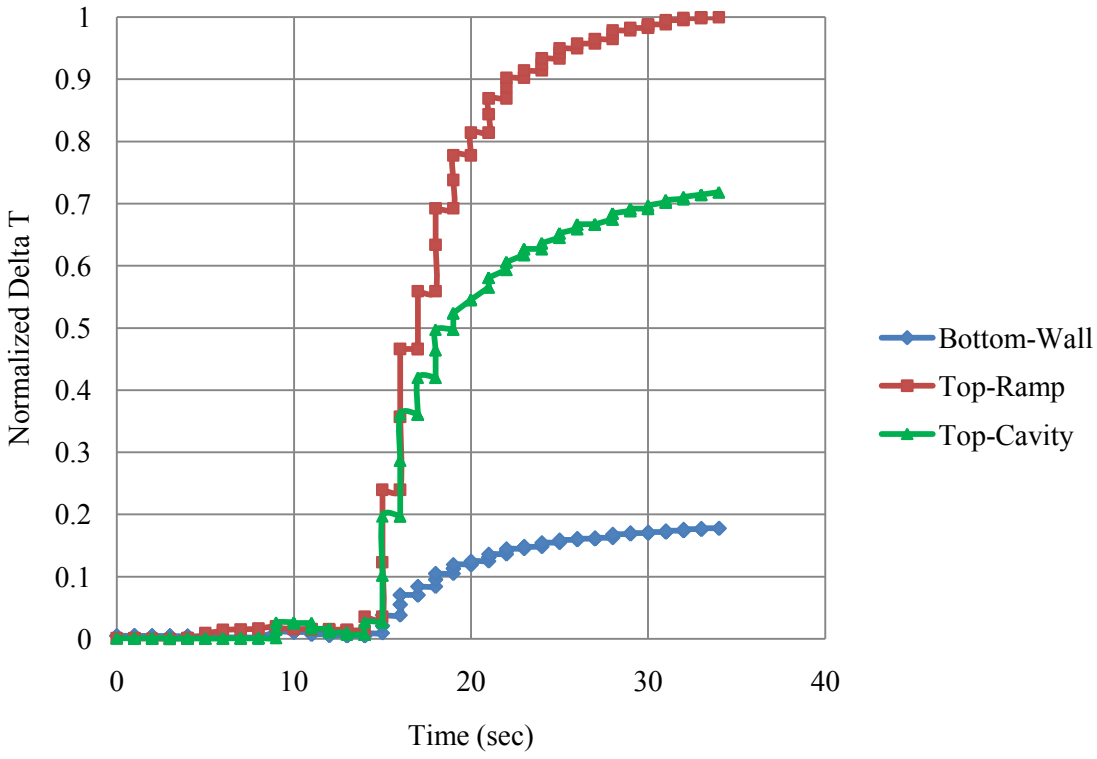

Figure 30: Cavity temperature for the single cavity run of case 5

The run had an equivalence ratio of 0.543 and used only I-2 fueling. The graph shows the greatest increases in temperature are inside the top cavity and at its ramp. This case is known to have combustion in the top cavity, so this temperature rise is expected. The wall directly below the cavity thermocouple on the bottom of the flow path also shows a small amount of temperature rise. The suggestion is some heat is making it to the bottom of the flow path. A likely cause is a temperature rise caused by the shock train.

Figure 31 shows the cavity temperatures for the dual cavity run from case 1. This run has similar conditions to the single cavity run from case 5 with an equivalence ratio of 0.583 and fueling from only I-2.

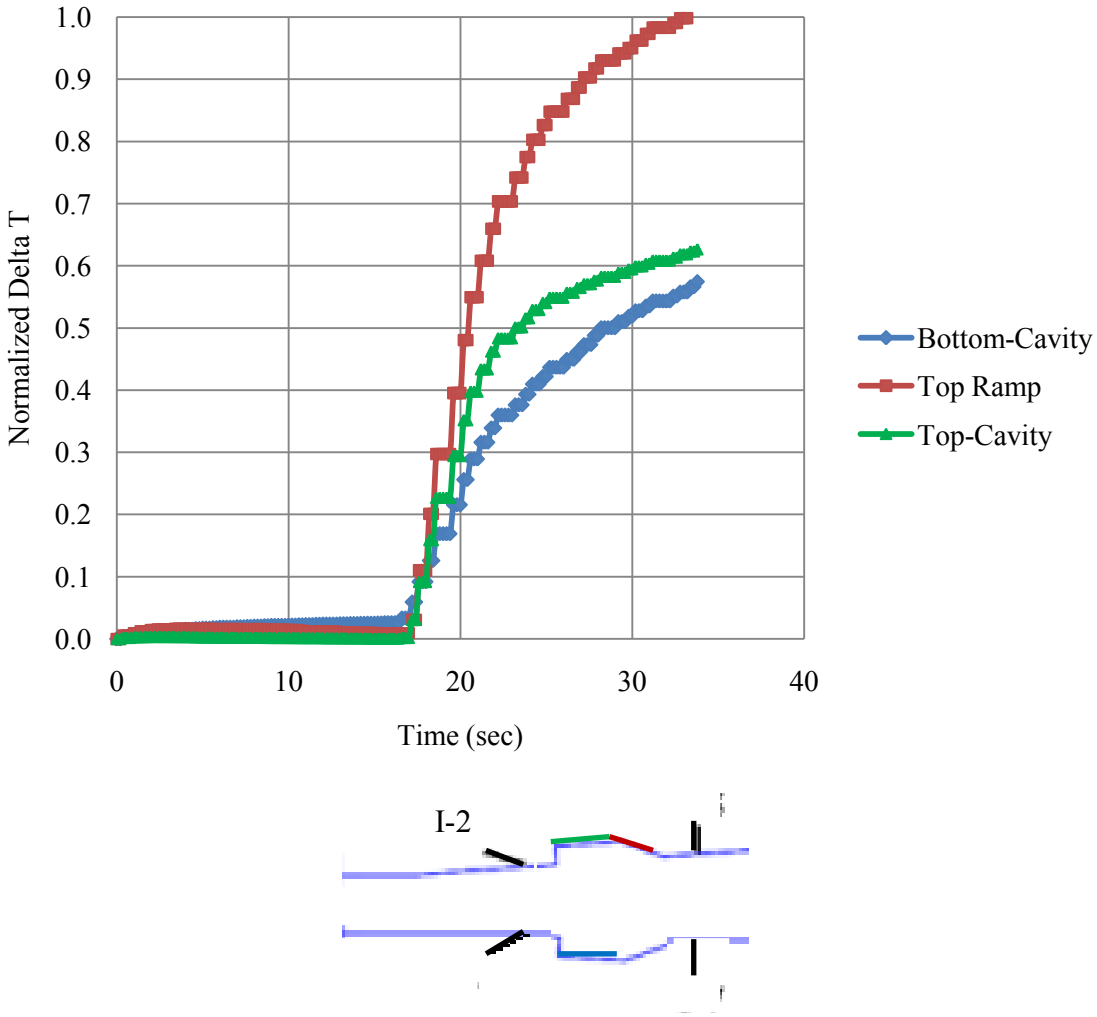

Figure 31: Cavity temperature for the dual cavity run of case 1 and thermocouple locations

This run shows the same trend for the top ramp and cavity. However, it shows a greater increase in bottom cavity temperature than was observed with the bottom wall without the cavity. This thermocouple is located lower in the flow path, sitting down inside of the cavity. If no combustion was taking place, the temperature would not be expected to have a larger increase at the bottom than the previous run. This result

suggests the possibility of some fuel migrating into the bottom cavity and combustion taking place there.

These two cases have only I-2 fueling. However, the dual cavity run of case 4 has a similar total equivalence ratio, but has fuel being injected from both I-2 and I-4. The cavity temperatures for this run are shown in Figure 32 below.

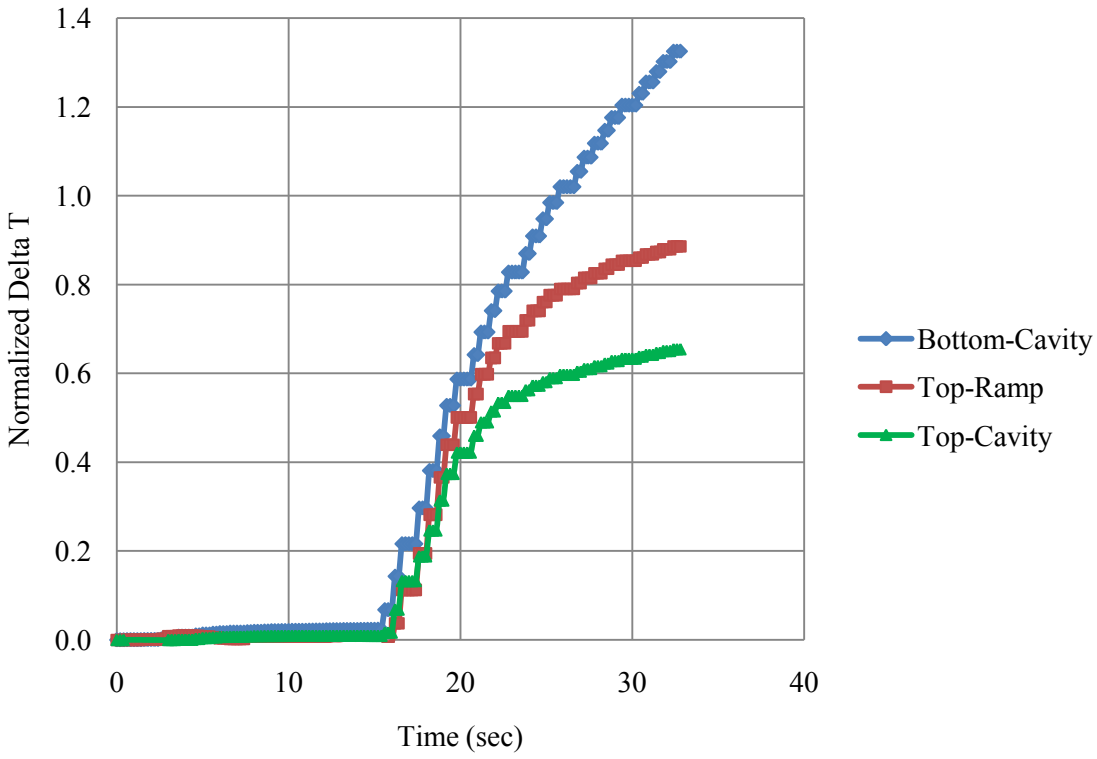

Figure 32: Cavity temperature for the dual cavity run of case 4

This case shows a slightly smaller increase in temperature on the top ramp and a similar temperature increase for the top cavity. This difference on the top is expected since only half of the fuel is now from I-2. However, the combustion taking place in the bottom cavity has caused the temperature to increase dramatically compared with case 1. Therefore, it is still difficult to determine exactly what is occuring in the bottom cavity in

the dual cavity run of case 1 and why the performance is increasing with the dual cavity when there is fueling from only I-2. Additional heat release is suspected of being responsible.

IV.9 CFD Analysis

The experimental results provide great insight into the combustion taking place in a dual cavity flow path. However, there are limitations to the instrumentation and flow visualization of this setup. Computational fluid dynamics (CFD) can help to further understand what is taking place inside the flow path.

CFD++, developed by Metacomp Technologies, was used for this study. A cubic κ-ε turbulence model and a gaseous ethylene chemistry kinetic model, based on the Princeton University 22-species reduced kinetic mechanism, was also used. A no-slip, adiabatic boundary condition was imposed on the solid walls. Due to the symmetry assumption at the center plane, only half of the scramjet isolator/combustor configuration was computed in this study.

There are a few issues contributing to the discrepancies between the numerical simulations and experimental data, including the adiabatic wall assumption, turbulence modeling, gaseous ethylene chemistry model and surface roughness. In the experiment, the scramjet flow path consists of a heat-sink rectangular isolator and a rectangular combustor. The interior surfaces of the entire flow path are covered with thermal barrier coating for additional thermal protection, which has a relatively rough surface. In addition, the combustor is water-cooled to protect the integrity of the material.

Since CFD uses the assumption of adiabatic boundary conditions, the numerical simulations do not account for the heat loss due to the water-cooled panels in the combustor section. In general, the numerical results will tend to over-predict the location of the leading edge of the shock train.

The two-equation turbulence models, such as the cubic κ-ε turbulence model, have ad hoc empirical constants, which might not be "fine-tuned" for the scramjet flow environment. In addition, the gaseous ethylene reduced kinetic model developed by Princeton University consists of 22 species and 206 elemental reactions, which is a reduction from the detailed ethylene oxidation mechanism with 70 species and 463 elementary reactions. Finally, the surface roughness due to the thermal barrier coating requires special wall treatment in the CFD approach to simulate the actual boundary layer growth. To avoid this complication, the present CFD calculation assumes a smooth interior surface.

The CFD pressure profiles for two runs are compared to the experimental results in Figure 33. Run 329AM is the single cavity run of case 1 with an equivalence ratio of 0.6 and I-2 fueling. Run 329AR is the dual cavity run from case 4 and has the same ER, but utilizes I-2 and I-4 fuel injection.

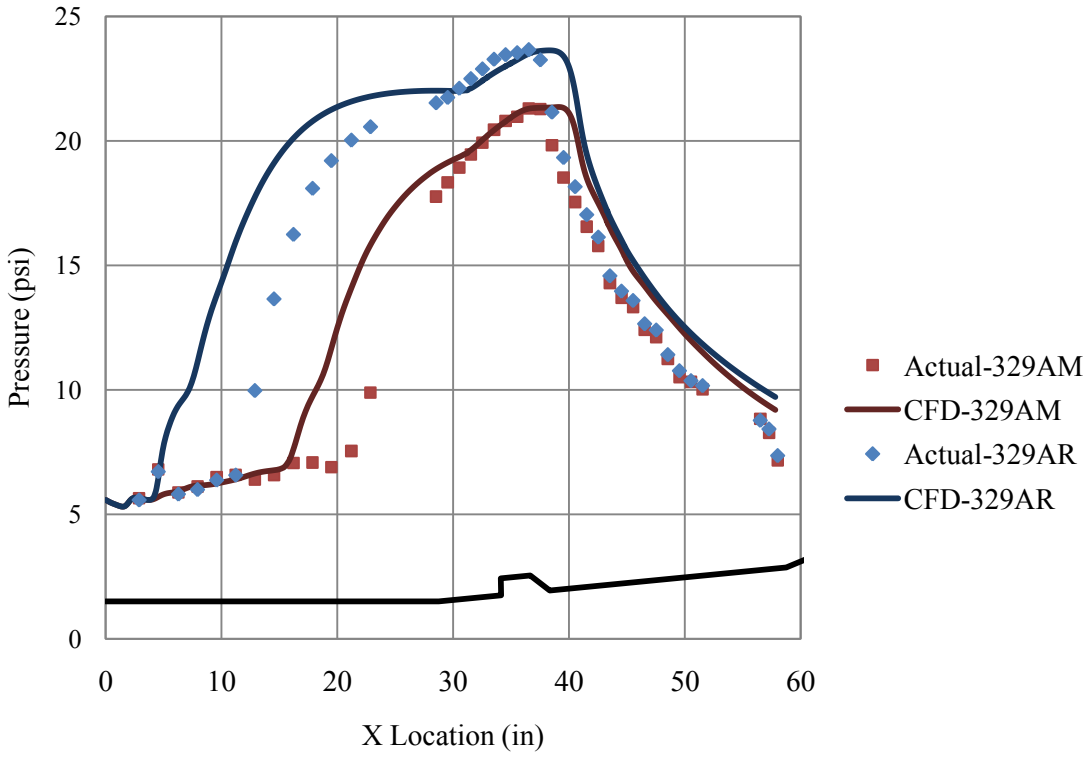

Figure 33: Experimental and CFD comparisons

The CFD shows very similar peak pressures as compared to the actual data. The CFD shows the position of the shock farther upstream, but the trends between CFD and the experimental profiles are very close. The overall trends are of greater importance in this study then actual temperatures and pressures. Therefore, the CFD is used as a supplement to the experimental results to further analyze the dual cavity performance.

In order to better understand why the dual cavity may be heating when the fuel is being injected from only I-2 on the top side, the equivalence ratio was studied. Figure 34 shows how the equivalence ratio may be changing throughout the flow path.

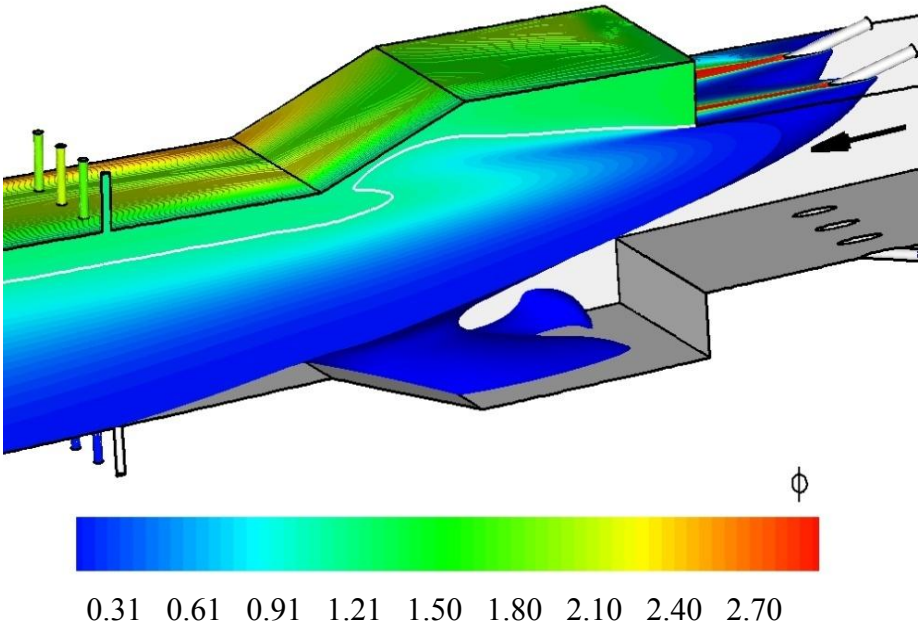

Figure 34: CFD equivalence ratio for the dual cavity run of case 1

The figure shows small amounts of fuel are reaching the bottom cavity. While the amount of fuel in the lower cavity would be very small, it is possible there would be enough for the cavity to light and for combustion to occur. CFD estimated the local equivalence ratio in the bottom cavity was approximately 0.06, well within the range for combustion to occur.

CFD can also verify the cavity temperature trends seen from the experimental test data. The CFD assumes adiabatic walls, so these temperatures are much higher than the experimental results. However, the trends are the same. Figure 35 shows the predicted static temperatures for the dual cavity run of case 1.

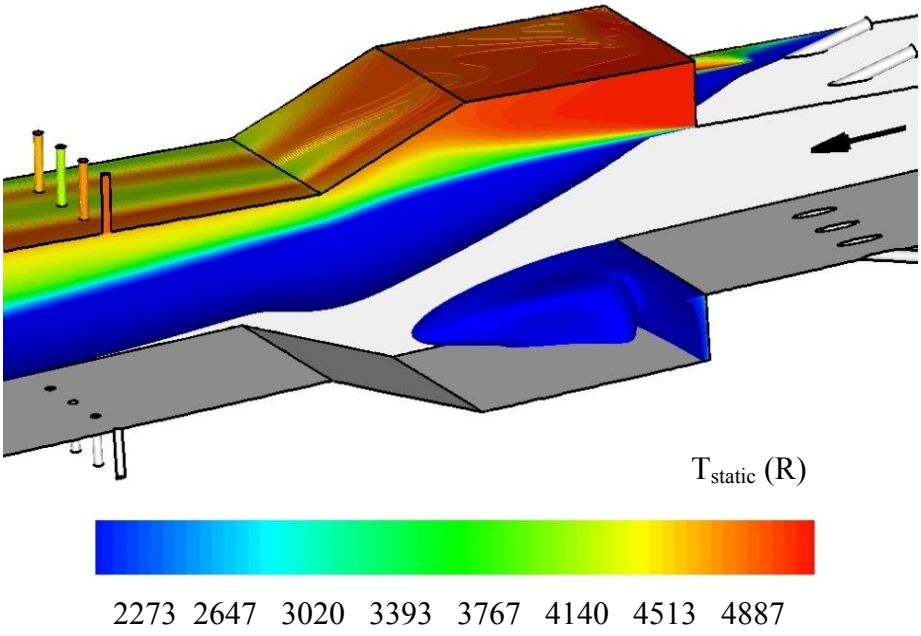

Figure 35: CFD temperature for the dual cavity run of case 1

The spark plug in the bottom cavity was simulated using a heat source on the cavity wall. The figure shows the highest temperatures occur in the top cavity as expected. However, there is still a temperature increase in the bottom cavity. These results support the experimental data showing the temperature rise in both cavities, not just the top.

It is expected that the heat rise is the bottom cavity is due to a small amount of combustion heating. This can be seen by the small concentration of OH in the bottom cavity in Figure 36.

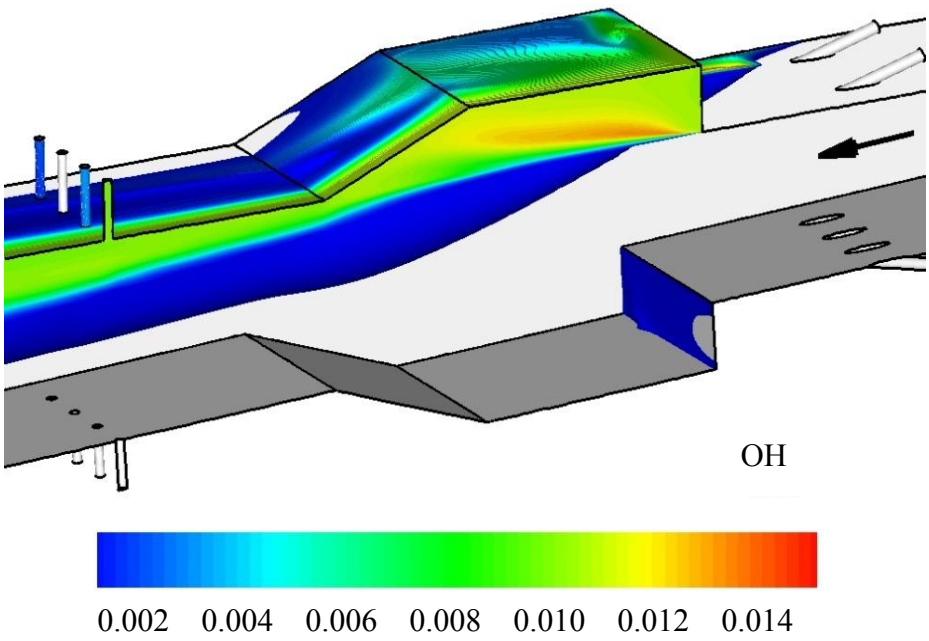

Figure 36: CFD OH concentration for the dual cavity run of case 1

Only areas of combustion should show increased OH concentrations. Significant combustion is also occurring in the top cavity, as expected. The CFD is helpful in verifying the experimental results as well predicting the cavity performance. Further investigation into CFD results would be beneficial in future studies.

IV.10 Digital and High Speed Photographs

The flow path was fitted with a quartz window in the combustor sidewall for one run night. This allowed flame emission images to be captured through digital and high speed photography. Similar fueling conditions were conducted as in the data runs described in Table 1. Figure 37 shows digital photographs of two dual cavity runs.

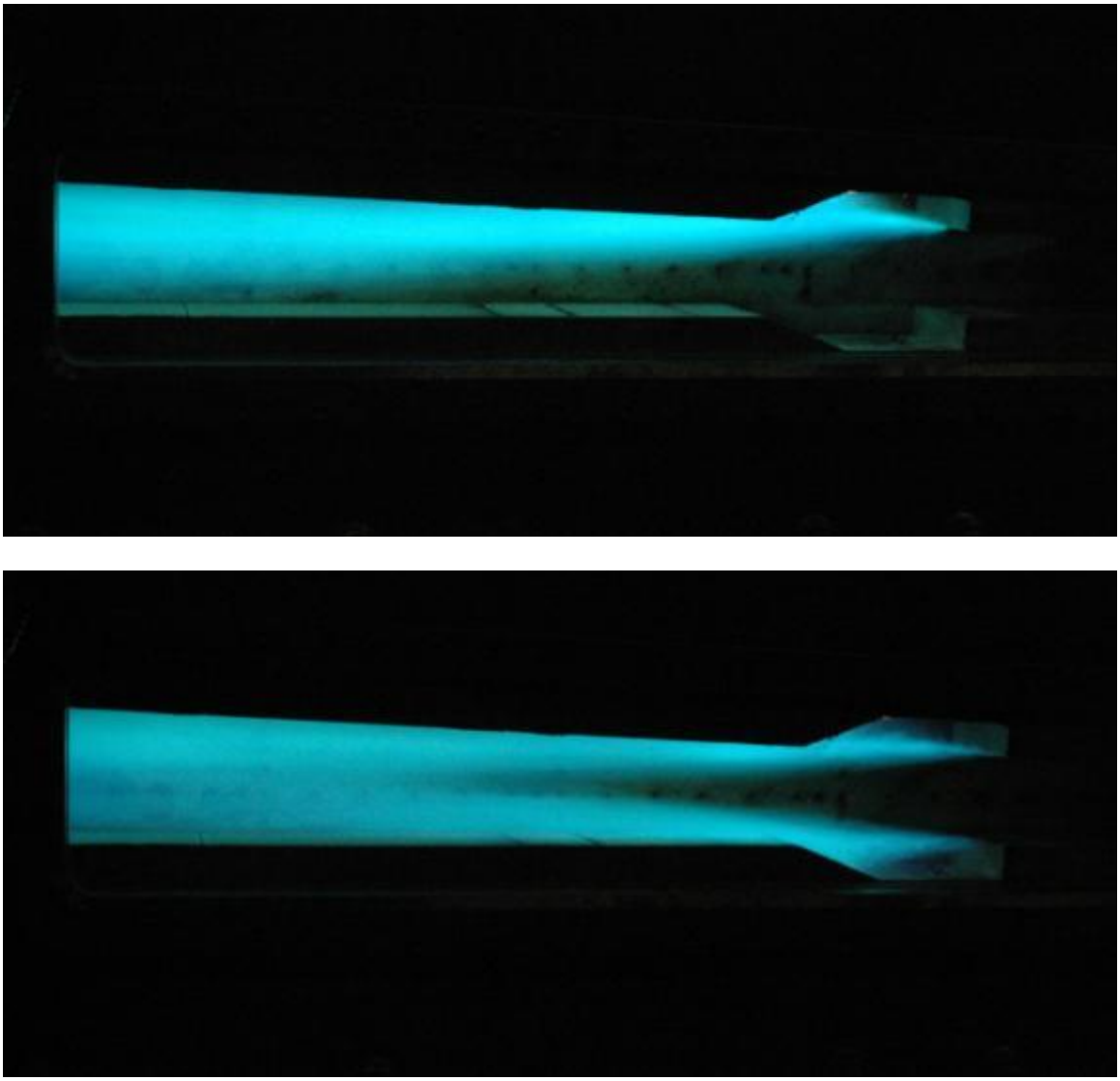

Figure 37: Digital photographs of combustion. Top: I-2 fueling only; Bottom: I-2 and I-4 fueling

The top photograph is combustion taking place with only I-2 fueling and an equivalence ratio of 0.61. The lower photograph has an equivalence ratio of 0.69 split equally between I-2 and I-4. This image shows combustion occurring in both cavities. These photographs give a better understanding of the combustion process and can verify when combustion is taking place in each of the cavities. The difference between top-only and top and bottom cavity fueling is clearly shown. However, there are limitations to what can be understood from this type of photograph. The images show illumination of the combustion across the entire flow path. The flame may be only near the combustor walls with a cold core. However, there is no way to tell at exactly what location in the flow the combustion is occurring.

Another method of visualization is through high-speed photography. The photos shown in Figure 38 were taken at 800 frames per second. The bottom picture shows a dual cavity run with fuel injection from I-2 and I-4 and an equivalence ratio of 0.3. It shows heat release in the cavities, but a cold core flow. The top photo is of a dual cavity run with only I-2 fueling and an equivalence ratio of 0.3. The combustion is primarily taking place in the top cavity. However, there is also heat release extended over half way down to the bottom cavity.

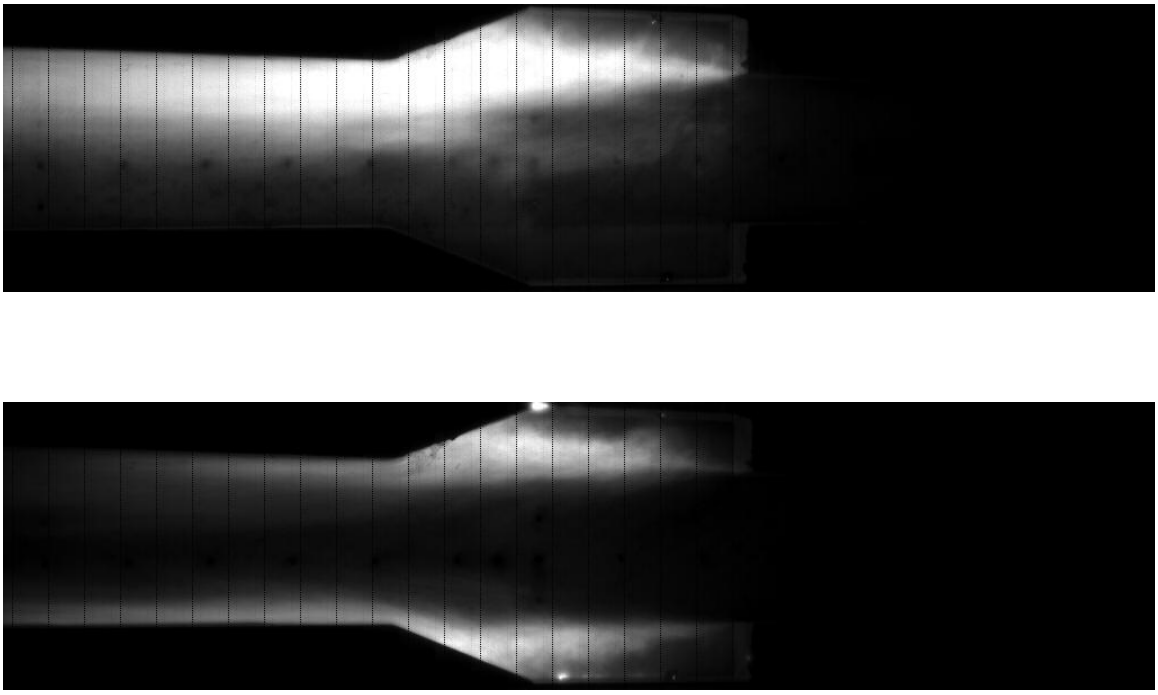

Figure 38: High-speed photographs. Top: I-2 injection only; Bottom: I-2 and I-4 injection

Figure 39 shows an additional timeframe of the I-2 only run.

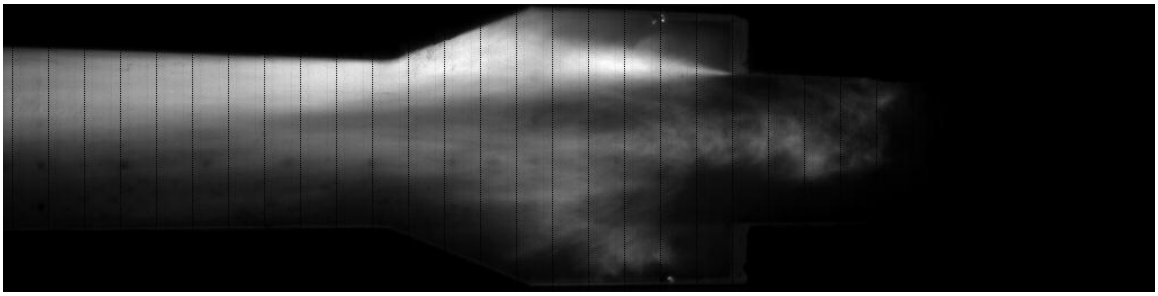

Figure 39: High-speed photograph showing combustion in bottom cavity using only I-2 injection

This photograph clearly suggests heat release in both cavities. While there is only fuel from the top, the CFD showed it is possible for fuel to be entrained into the bottom

cavity, most likely through sidewall interaction. There are spark plugs in both cavities which allow them to be lit simultaneously, even when fuel is only being injected from I-2. It is likely that fuel is traveling down the sidewall of the combustor where there are lower flow velocities. Small amounts of fuel are creeping into the cavity, being ignited, and burning for short periods of time. The flow in this area varies greatly with time, but this photo is evidence that it is possible for the bottom cavity to light with only I-2 fuel injection. These photos explain why the dual cavity provides better performance, higher pressures and temperatures, and higher stream thrusts as compared to similar conditions with only a single cavity flame holder.

V Conclusions and Recommendations

V.1 Conclusions

The first objective of this study was to investigate the dual cavity performance and to determine the advantages and disadvantages of using a dual cavity versus a single cavity flame holder. This objective was accomplished by studying wall pressures, temperatures, pressure ratios, stream thrusts, combustion efficiencies, CFD, and visualization.

Peak pressure and combustor exit pressures were studied and the dual cavity consistently showed higher ratios for both. The increase in pressure is a result of additional heat being released from the combustion process. This result suggests the dual cavity flow path provides better combustion and performance than the single cavity.

Stream thrust was the next performance parameter studied. Each case showed a stream thrust significantly higher for the dual cavity than for the single cavity. The dual flow path had an average of 34% higher values over all of the cases. The increase of stream thrust with the dual cavity is further evidence that adding the additional flame holder provides better performance.

The combustion efficiency was the final performance parameter studied. Unlike the pressures ratios and stream thrusts, the efficiencies failed to show any consistent trend. After analysis of the first two parameters, higher combustion efficiencies would also be expected from the dual cavity. There are several uncertainties in the way the combustion efficiency is calculated which could cause the inconsistent results. The current method of analysis needs to be further refined. At this time, the combustion

efficiencies found in this study are unreliable. Additional verification of the process may provide results that are more consistent in the future.

The second objective of this study was to investigate the operability of the dual cavity flow path over a range of equivalence ratios and fuel injection schemes. Each run with the dual cavity configuration had a shock position farther upstream in the isolator than the single cavity flow path. The dual cavity had a smaller range of operability and proved to be more likely to unstart as the equivalence ratio was increased to 1.0 or higher. Including bottom side injection also moved the pre-combustion shock train further upstream and decreased the operability range of the dual cavity.

The final objective was to analyze the overall advantages and disadvantages of the two flow path configurations and to determine if the dual cavity flame holder may be a viable option for future scramjet engines. The single cavity flow path has been more extensively studied in the past and is known to provide sufficient combustion under most conditions. This research verified operability of the single cavity flow path between equivalence ratios of approximately 0.53 to 0.95. The operability window of the dual cavity flow path was smaller than that of the single cavity as the equivalence ratio was increased. However, the dual cavity did provide increased overall performance shown by the stream thrust and pressure ratio results. The analysis conducted in this study suggests the dual cavity flame holder flow path provides significant advantages over the baseline and would be a viable option for future scramjet engines. However, the flight conditions and equivalence ratios could provide limitations to its capabilities. Operational equivalence ratios range from approximately 0.3 to 1.2. Fuel rich conditions are useful during periods of acceleration where maximum thrust is desired. The inability to operate

with these high equivalence ratios could increase acceleration time, thereby reducing cruise speed, flight time, and range.

V.2 Recommendations

Further study of these parameters and additional investigation into the processes used would provide clarification and repeatability of these results as discussed below. Recommendations for future work include analysis of the data from additional runs, verification of the QPERF code used to determine combustion efficiency, further CFD modeling, reorganization of data output processes, and further testing of alternate fueling and flight conditions.

There were 216 runs conducted during this study, and only 14 were fully analyzed. There is an enormous amount of data ready to be studied. An entire set of data with the Mach 1.8 nozzle was acquired but only briefly looked at. There are also runs with additional fuel injection sites and a wider range of equivalence ratios yet to be analyzed. This further analysis will likely provide confirmation of the results discovered in this research.

The combustion efficiency found using the in-house code QPERF was the only parameter disagreeing with the rest of the results. While all other performance parameters suggested the dual cavity would provide better performance, the combustion efficiency was largely indifferent. QPERF makes several assumptions that can lead to inaccuracies. The combustion efficiencies output are highly dependent on the ambient pressure, base pressure, exit pressure, load cell force, and the width of the combustor, as well as many

other parameters (13). The ambient pressure, the load cell forces, and the width of the combustor are all known to a high degree of accuracy. However, the base and exit pressures used by the code are not necessarily calculated in the most accurate way. First, the exit pressure is based off of the reading from one pressure tap on the top wall of the truncated nozzle. The pressure in this region can vary greatly from top to bottom. This is especially true when there is combustion on only one side of the flow path. For example, the single cavity run from case 6 has a top side exit pressure of 8.88 psia and a bottom side pressure of 7.67 psia. A more accurate calculation for efficiency would use an average of pressure tap readings from both the top and bottom walls. The base pressure is also a concern. It is calculated as an average of 12 pressure tap readings from all sides of the flow path. However, the value does not take into consideration the area from each pressure tap. The taps are not evenly distributed around each portion of the flow path, especially around the corners, and this could have a substantial effect on the value. A more accurate value could be found by taking an area-weighted average of all twelve pressure taps. This would ensure each area is accounted for properly. These items, as well as overall testing and verification of the code, are suggested as future work. Once the code is known to provide accurate results, the data from these cases should be rerun and studied. New results may provide confirmation of the improved performance with the dual cavity.

Computational fluid dynamics models can provide valuable insight into combustion processes. Due to the limited scope of this study, only a small amount of CFD results were analyzed. This analysis can be useful for determining how the fuel is being mixed, what temperatures are being seen and how well the flow is burning. CFD

can also be used to look at additional conditions, equivalence ratios, and fuel injections schemes not physically tested in the rig. The CFD models should be used to provide repeatability of the dual cavity performance seen in this study as well as to provide information on conditions not yet considered, such as additional Mach number ranges, flight conditions, and fuel injection schemes.

The large amount of data acquired per run can become overwhelming for analysis purposes. With approximately 1300 data elements output over an average of 20,000 time samples for each run night, the hand computed filtering process can become extremely time consuming. Organizing the outputs into a more user-friendly form would make the analysis process more convenient. For example, the pressure ports could be organized according to their axial position along the flow path. If the analysis process could be simplified, many more runs could be analyzed for the performance and operability characteristics studied in this research. It is important to look at these additional runs as the flow path will behave differently under each condition. Automation of the data reduction process and improved data processing algorithms would be a significant time saver.

Finally, further testing could be conducted using additional fuel injection schemes and flight conditions. This would allow performance and operability trends to be established for conditions that were not specifically looked at in this study. Performance trends are not necessarily linear, and therefore require numerous data points to ensure accurate results are established throughout the entire range of conditions. It would also be beneficial to test fuels that are less reactive than ethylene, such as ethylene-methane mixtures or JP fuels, since ethylene will not be used in actual flight vehicles.

There are hundreds of possible test conditions for this configuration that could potentially be conducted.

V.3 Research Question

This research was conducted in order to answer the question: does a dual cavity flow path hold significant advantages over a similar flow path with only a single cavity flame holder? Yes, from this initial study, the dual cavity flame holder has proven its potential to provide improved performance for a reliable scramjet engine.

VI Bibliography

1. Dolvin, Douglas J., "Hypersonic International Flight Research Experimentation (HIFiRE) Fundamental Sciences and Technology Development Strategy," AIAA Paper 2008-2581. 2008.

2. Andreadis, Dean. Tip Magazine. Scramjets Integrate Air and Space. [Online] July 24, 2004. [Cited: May 4, 2009.] http://www.tipmagazine.com/tip/INPHFA/vol-10/iss-4/p24.pdf.

3. Gruber, Mark, Jackson, Kevin, Jackson, Thomas and Liu, Jiwen, "Hydrocarbon-Fueled Scramjet Combustion Flowpath Development for Mach 6-8 HIFiRE Flight Experiments," JANNAF Paper. 2008.

4. Lin, Kuo-Cheng, Tam, Chung-Jen, Boxx, Isaac, Carter, Campbell, Jackson, Kevin and Lindsey, Martin, "Flame Characteristics and Fuel Entrainment Inside a Cavity Flame Holder in a Scramjet Combustor," AIAA Paper 2007-5381. 2007.

5. Liu, Jiwen, Tam, Chung-Jen, Lu, Tianfeng and Law, Chung K., "Simulations of Cavity-Stabilized Flames in Supersonic Flows Using Reduced Chemical Kinetic Mechanisms," AIAA Paper 2006-4862. 2006.

6. Ben-Yakar, Adela and Hanson, Ronald K., "Cavity Flameholders For Ignition and Flame Stabilization in Scramjets: Review and Experimental Study," AIAA Paper 1998-3122. 1998.

7. Ben-Yakar, Adela, "Cavity Flame-Holders for Ignition and Flame Stabilization in Scramjets: An Overview," Journal of Propulsion and Power. 2001.

8. Gruber, M. R., Donbar, J. M., Carter, C. D. and Hsu, K. -Y., "Mixing and Combustion Studies Using Cavity-Based Flameholders in a Supersonic Flow," Journal of Propulsion and Power. 2004. Vol. 20, 5.

9. Haubelt, Lane C., "Performance of Pylons Upstream of a Cavity-based Flameholder in Non-reacting Supersonic Flow," AIAA Paper 2006-4679. 2006.

10. Mathur, Tarun, Gruber, Mark, Jackson, Kevin, Donbar, Jeff, Donaldson, Wayne, Jackson, Thomas and Billig, Fred, "Supersonic Combustion Experiments with a Cavity-Based Fuel Injector," Journal of Propulsion and Power. 2001. Vol. 17, 6.

11. Huellmantel, L. W., Ziemer, R. W. and Cambel, A. B., "Stabilization of Premixed Propane-Air Flames in Recessed Ducts," Jet Propulsion. 1957. pp. 31-43.

12. Lin, Kuo-Cheng, Jackson, Kevin, Behdadnia, Robert, Jackson, Thomas A., Ma, Fuhua, Li, Jian and Yang, Vigor, "Acoustic Characterization of an Ethylene-Fueled Scramjet Combustor with a Recessed Cavity Flameholder," AIAA Paper 2007-5382. 2007.

13. Smith, S., Scheid, A., Eklund, D., Gruber, M., Wilkin, H. and Mathur, T., "Supersonic Combustion Research Laboratory Uncertainty Analysis," AIAA Paper 2008-5065. 2008.

14. Esterline Pressure Systems. [Online] [Cited: May 7, 2009.] http://www.pressuresystems.com/9816-rk1.html.

15. Gruber, Mark, Carter, Campbell, Ryan, Michael, Rieker, Gregory B., Jeffries, Jay B., Hanson, Ronald K., Liu, Jiwen and Mathur, Tarun, "Laser-Based Measurements of OH, Temperature, and Water Vapor Concentration in a Hydrocarbon-Fueled Scramjet," AIAA Paper 2008-5070. 2008.

Vita

First Lieutenant MacKenzie J. Collatz graduated from Bloomington Jefferson High School in Bloomington, Minnesota in 2001. She then enrolled at the University of Minnesota-Twin Cities where she graduated with a Bachelor of Science degree in Aerospace Engineering. She earned her commission in the United States Air Force through the Reserve Officer Training Corps program in 2006. She then entered active duty and began work at the Propulsion Directorate of the Air Force Research Laboratory at Wright-Patterson Air Force Base in Dayton, Ohio. She pursued her Master's of Science degree in Space Systems as a part time student at the Air Force Institute of Technology and will graduate in June of 2009.

REPORT DOCUMENTATION PAGE

Form Approved
OMB No. 074-0188

1. REPORT DATE *(DD-MM-YYYY)*	**2. REPORT TYPE**	**3. DATES COVERED** *(From – To)*
08-06-2009	Master's Thesis	Sept 2008 – Jun 2009

4. TITLE AND SUBTITLE

Performance and Operability of A Dual Cavity Flame Holder In A Superonsic Combustor

5a. CONTRACT NUMBER

5b. GRANT NUMBER

5c. PROGRAM ELEMENT NUMBER

6. AUTHOR(S)

Collatz, MacKenzie J., First Lieutenant, USAF

5d. PROJECT NUMBER
N/A

5e. TASK NUMBER

5f. WORK UNIT NUMBER

7. PERFORMING ORGANIZATION NAMES(S) AND ADDRESS(S)
Air Force Institute of Technology
Graduate School of Engineering and Management (AFIT/EN)
2950 Hobson Way, Building 640
WPAFB OH 45433-8865

8. PERFORMING ORGANIZATION REPORT NUMBER

AFIT/GSS/ENY/09-J01

9. SPONSORING/MONITORING AGENCY NAME(S) AND ADDRESS(ES)
Dr. Mark Gruber
Aerospace Propulsion Division
1950 Fifth Street (937) 255-7350
WPAFB, OH 45433 mark.gruber@wpafb.af.mil

10. SPONSOR/MONITOR'S ACRONYM(S)
AFRL/RZA

11. SPONSOR/MONITOR'S REPORT NUMBER(S)

12. DISTRIBUTION/AVAILABILITY STATEMENT

APPROVED FOR PUBLIC RELEASE; DISTRIBUTION UNLIMITED.

13. SUPPLEMENTARY NOTES

14. ABSTRACT
The current generation of hydrocarbon fueled scramjet combustors typically requires a flame holding device to facilitate flame ignition and stable combustion. The amount of time available for fuel injection, fuel-air mixing, and combustion is very short, on the order of 1 millisecond. This short dwell time, along with the relatively long ignition delay times of hydrocarbon fuels, makes the flow path and flame holder design extremely important. This study investigates the performance and operability of using a symmetric dual cavity flame holder flow path to stabilize and enhance supersonic combustion. Testing of this flow path configuration, as well as a baseline single cavity flow path, was conducted in Research Cell 18 of the Propulsion Directorate at the Air Force Research Laboratory (AFRL/RZ). Performance and operability of the flow paths were determined through analysis of wall pressures, temperatures, pressure ratios, stream thrusts, combustion efficiencies, computational fluid dynamics, and visualization. The dual cavity flame holder showed a significant overall increase in performance through higher temperatures, pressure ratios, and stream thrusts. This research has proven the potential of a dual cavity flame holder to provide improved performance for a reliable scramjet engine.

15. SUBJECT TERMS
Scramjet, Supersonic Combustion, Dual Cavity, Fuel Injection, Combustion Efficiency

16. SECURITY CLASSIFICATION OF:			**17. LIMITATION OF ABSTRACT**	**18. NUMBER OF PAGES**	**19a. NAME OF RESPONSIBLE PERSON**
a. REPORT	**b. ABSTRACT**	**c. THIS PAGE**			Richard Branam, Lt Col, USAF
U	**U**	**U**	**UU**	85	**19b. TELEPHONE NUMBER** *(Include area code)* (937) 255-6565, ext 7485 (richard.branam@afit.edu)

Standard Form 298 (Rev. 8-98)
Prescribed by ANSI Std. Z39-18